

APPENDICES

ลิขสิทธิ์มหาวิทยาลัยเชียงใหม่

Copyright © by Chiang Mai University

All rights reserved

APPENDIX A

THEORY OF PURITY ANALYSIS (STANDARD METHOD OF CALCULATION)

The purity of an organic compound can be quantitatively determined by DSC. If a material contains even a minute amount of an impurity, its melting point (T_m) is depressed from that of the infinitely pure material (T_0) and its melting range is broadened. The degree of melting point depression ($T_0 - T_m$) depends upon the amount of impurity as follows [115]:

$$(T_0 - T_m) = \frac{RT_0^2 X_2}{\Delta H_m} \quad (1)$$

where:

R = molar gas constant, $8.314 \text{ J K}^{-1} \text{ mol}^{-1}$

X_2 = mole fraction of impurity

ΔH_m = heat of melting, J mol^{-1}

From a DSC scan of a sample, its melting point depression can be determined from:

$$F = \frac{T_0 - T_m}{T_0 - T_s} \quad (2)$$

where

F = fraction melted

T_s = sample temperature at any point as read from the DSC curve

Rearranging this equation gives:

$$T_s = T_0 - \frac{(T_0 - T_m)}{F} \quad (3)$$

Substituting Equation 1, which defines the melting point depression due to an impurity, into Equation 3, yields a linear relationship between T_s and $1/F$ as shown in Equation 4:

$$T_s = T_0 - \left(\frac{RT_0^2 X_2}{\Delta H_m} \right) \times \frac{1}{F} \quad (4)$$

This equation is known as the Van't Hoff Equation. Since Equation 4 is a linear relationship, a plot of the sample temperature (T_s) on the Y-axis versus the reciprocal of the fraction of material melted at that temperature ($1/F$) on the X-axis should give a straight line with a slope equal to the melting point depression ($\text{slope} = -RT_0^2 X_2 / \Delta H_m$) and a Y-intercept = T_0 (at $1/F = 0$). This linear plot is referred to as a Van't Hoff plot. The fraction of material melted at any sample temperature is determined directly from the dynamic DSC scan and is proportional to the peak area under the curve up to that temperature. By generating this Van't Hoff plot from a series of sample temperatures in the range from approximately 6 to 59 % melted, it is a relatively simple procedure to determine T_0 from the intercept of the line. Finally, the mole fraction of impurity is calculated from the slope. However, in practice, the experimental results deviate somewhat from the theory with the result that a correction has to be made using the relation below:

$$F = \frac{\Delta H_s + X}{\Delta H_m + X} \quad (5)$$

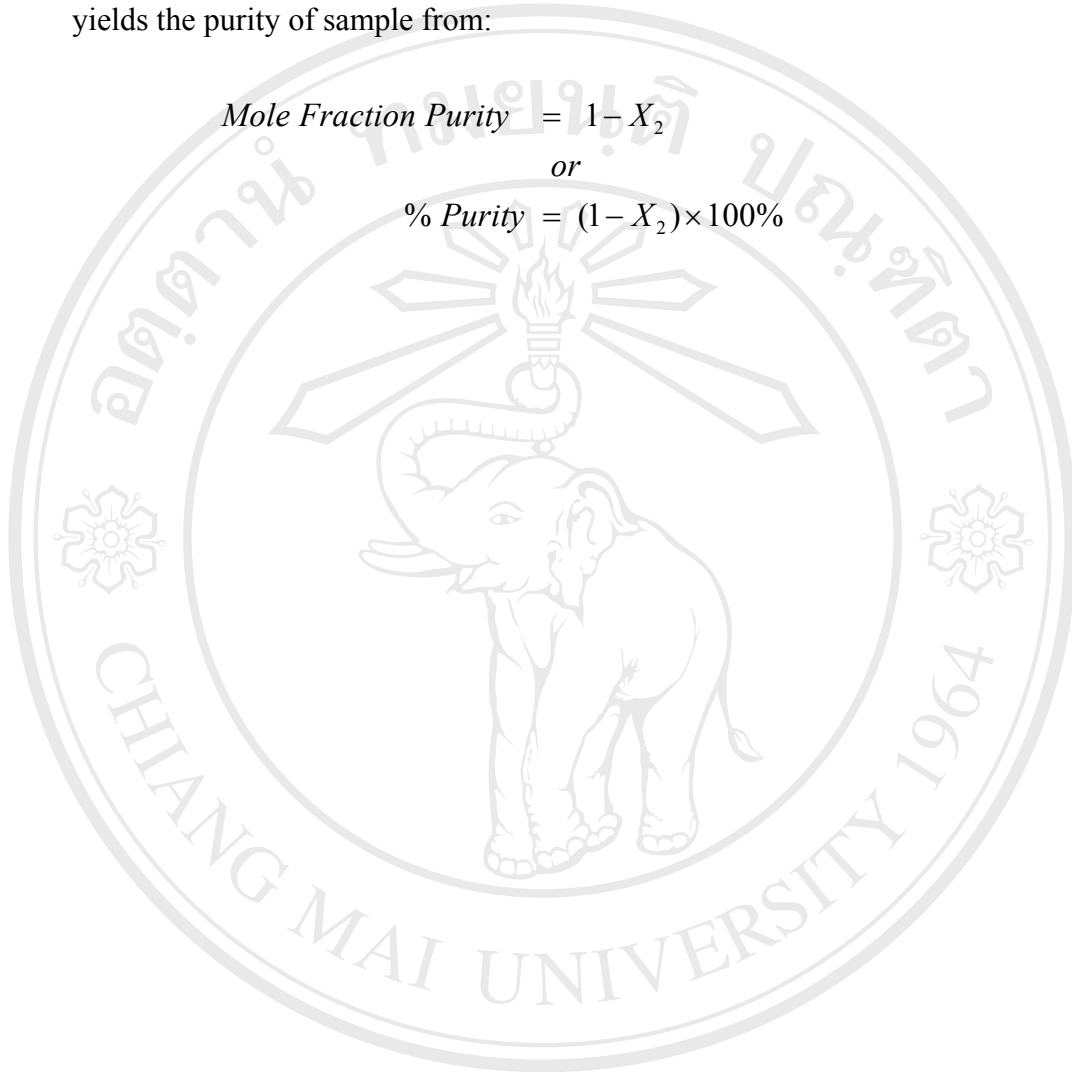
where

ΔH_s = heat of melting up to temperature, T_s

X = a constant for fitting the raw data to a straight line

After making this correction, one can now convert the raw data to fit the theoretically straight line predicted by the Van't Hoff equation. The calculated value of X_2 then yields the purity of sample from:

$$\begin{aligned} \text{Mole Fraction Purity} &= 1 - X_2 \\ \text{or} & \\ \% \text{ Purity} &= (1 - X_2) \times 100\% \end{aligned} \quad (6)$$



ลิขสิทธิ์มหาวิทยาลัยเชียงใหม่
Copyright © by Chiang Mai University
All rights reserved

APPENDIX B

SUPPORTING PAPERS

Conference Presentations

1. Comparison of Crystallisation Kinetics of Random Terpolymer and Segmented Triblock Terpolymer Fibres based on L-lactide, ϵ -Caprolactone and Glycolide
W. Channuan, J. Siripitayananon, R. Molloy, Y. Baimark
Biennial Polymer Conference : Polymer Physics Group,
10th-12th September 2003, University of Reading, Reading, UK
2. Investigation of the Crystal Structure in Segmented Triblock L-lactide, ϵ -Caprolactone and Glycolide Terpolymer Fibres
W. Channuan, J. Siripitayananon, R. Molloy, M. Sriyai, G. R. Mitchell
International Conference on Smart Materials: Smart/Intelligent Materials and Nanotechnology
1st-3rd December 2004, Chiang Mai, Thailand
3. Structural Characterisation of Crystallisable Terpolymers of L-lactide, ϵ -Caprolactone and Glycolide
W. Channuan, J. Siripitayananon, R. Molloy, M. Sriyai and G. R. Mitchell
The Fourth Thailand Materials Science and Technology Conference
31st March–1st April, 2006, Thailand Science Park Convention Center, Thailand

Journal Publications

1. The Structure of Crystallizable Copolymers of L-lactide, ϵ -Caprolactone and Glycolide
W. Channuan, J. Siripitayananon, R. Molloy, M. Sriyai, F. J. Davis and G. R. Mitchell, *Polymer*, 2005, 46: 6411.
2. Investigation of the Crystal Structure in Segmented Triblock L-lactide, ϵ -Caprolactone and Glycolide Terpolymer Fibres
W. Channuan, J. Siripitayananon, R. Molloy, M. Sriyai, G. R. mitchell, *Chiang Mai J. Sci.*, 2005, 32(3): 507.

CONFERENCE PRESENTATIONS

in

**Biennial Polymer Conference
Polymer Physics Group**

held at

**University of Reading
Reading, UK**

ลิขสิทธิ์มหาวิทยาลัยเชียงใหม่
Copyright © by Chiang Mai University
All rights reserved

10th-12th September 2003



UNIVERSITY OF READING
POLYMER SCIENCE CENTRE

Biennial Polymer Conference

POLYMER PHYSICS GROUP

**The Institute of Physics
The Royal Society of Chemistry
The Institute of Materials, Minerals and Mining.**

10th – 12th September 2003.

ลิขสิทธิ์มหาวิทยาลัยเชียงใหม่

Copyright © Chiang Mai University

All rights reserved

COMPARISON OF CRYSTALLISATION KINETICS OF RANDOM TERPOLYMER AND SEGMENTED TRIBLOCK TERPOLYMER FIBRES BASED ON L-LACTIDE, ϵ -CAPROLACTONE AND GLYCOLIDE.

W. Channuan, J. Siripitayananon, R. Molloy and Y. Baimark
Biomedical Polymers Research Unit, Department of Chemistry,
Faculty of Science Chiang Mai University, 50200 Thailand

G.R. Mitchell

Polymer Science Centre and Department of Physics, University of Reading
Whiteknights, Reading RG6 6AF UK

The objective of this proposed research is to develop a new synthetic monofilament fibre with the appropriate balance of physical and mechanical properties for use as an absorbable surgical suture. The polyesters of particular interest in this research are terpolymers based on L-lactide (LL), ϵ -caprolactone (CL) and glycolide (G). Random and segmented triblock terpolymers with the same composition ratio of LL : CL : G = 70 : 25 : 5 mole % were synthesized via ring opening bulk polymerization [1,2]. The terpolymers were melt-spun into cooled water bath (5 – 10 °C) to produce amorphous as-spun monofilament fibre. The as-spun fibres were then hot-drawn under various conditions to enhance mechanical properties. We had studied crystallisation rates of as-spun fibres of both terpolymers x-ray diffraction techniques. It was found that crystallisation rates of segmented triblock terpolymer occurred much faster than the random terpolymer. We have compared the quiescent crystallisation rate with those observe during the hot drawing stage using in-situ WAX techniques, coupled with a miniature hot drawing stage. We found that the mechanical properties of the fibre are strongly related to the morphology and structure, which develop during hot drawing. We have used the in-situ x-ray scattering to prepare a processing scheme which yields optimum properties.

[1] M. Srisa-ard, R. Molloy, N. Molloy, J. Siripitayananon and M. Sriyai, **Polym. Int** 2001; 50:8, 891-896.

[2] Q. Cai, J. Bei, S. Wang, **Polym. Adv. Technol.** 2000; 11: 159-166.



COMPARISON OF CRYSTALLIZATION OF RANDOM TERPOLYMER AND SEGMENTED TRIBLOCK TERPOLYMER FIBRES BASED ON L-LACTIDE, ϵ -CAPROLACTONE AND GLYCOLIDE

W. Channuan, J. Siripitayanon, R. Molloy and Y. Baimark

Biomedical Polymers Research Unit, Department of Chemistry, Faculty of Science
Chiang Mai University, 50200 Thailand

G. R. Mitchell

Polymer Science Centre and Department of Physics, University of Reading
Whiteknights, Reading RG6 6AF UK

Introduction

Synthetic biodegradable polyesters have the advantage over natural materials in that they can be tailored to give a wider range of properties. They have been widely used for many biomedical purposes. In this research, attention is focused on suture applications. We try to develop a new synthetic monofilament fibre with the appropriate balance of physical and mechanical properties for use as an absorbable surgical suture.

Experimental

Synthesis and Characterisation

There are two type of terpolymers used in this study [1,2].

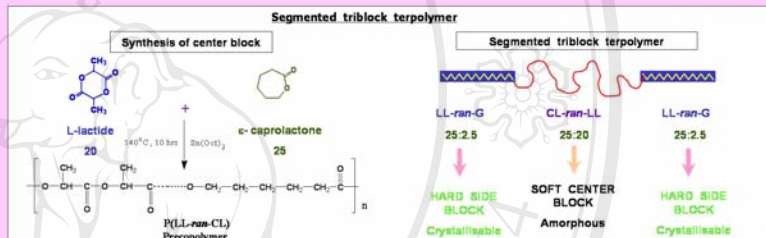
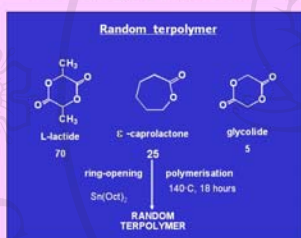


Table 1. Characteristics of Random terpolymer and block terpolymer

Polymer	Intrinsic viscosity, $[\eta]$ (dl/g)	Mw	Mn	Mw/Mn	Tg	Tm	Td
Random terpolymer	1.27	61,000	33,000	1.85	44.5	149.9	252
Segmented triblock terpolymer	0.98	47,000	27,439	1.71	47	159	254

Fibre processing

The processing equipment to be used is a small-scale melt spinning apparatus [3].

The segmented triblock terpolymer was to be melted at 167 °C.

Random terpolymer was melt-spun at 150 °C.



Fig 1 Schematic diagram of the small-scale melt spinning apparatus

Results

1. Rate of crystallization

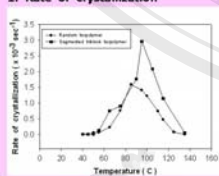


Fig 2. Rate of crystallization

2. X-ray diffraction patterns of fibres drawn at various conditions indicate different orientations

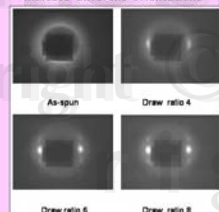


Fig 3. WAXS patterns of random terpolymer at different draw ratios at 40 °C

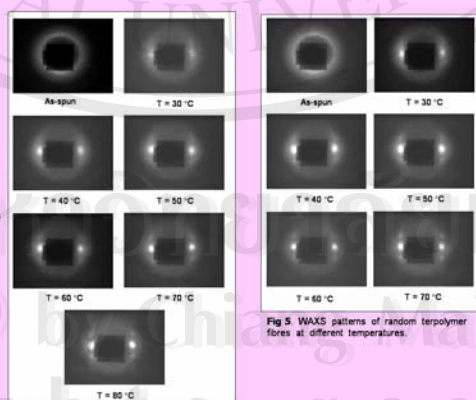


Fig 4. WAXS patterns of segmented triblock terpolymer fibres at different temperatures.

WAXS

The X-ray measurements were carried out with Cu K α radiation at a wavelength of 1.542 Å. The instrument was operated at 40 kV and 20 mV with a collimator size of 1 mm. For WAXS technique, the fibre sample was closely aligned in parallel to cover a hole 5 mm in diameter in a metal plate. The plate was the mounted on a goniometer, normal to the X-ray beam. By using a flat area detector, each sample was exposure 30 secs.

X-ray Diffractometer

X-ray diffractometer operates with a Cu targeted tube at $\lambda = 1.54178 \text{ \AA}$ with an incident beam graphite monochromator. The instrument utilizes a Philips generator operating at 40 kV and 40 mA with a collimator size of 1.0 mm. For studying isothermal crystallization of terpolymer. The fiber sample was packed in the capillary tube that has diameter size 2 mm. It was mounted on a goniometer. The data were collected at constant temperatures.

Conclusion

It was found that crystallisation rates of segmented triblock terpolymer occurred much faster than the random terpolymer.

Further work

We have planned to investigate morphology development in fibre during hot-drawing using in-situ X-ray scattering diffraction technique.

Acknowledgements

This work was supported by the National Metal and Materials Technology Center of Thailand (MTEC). W.C. Would like to thank the Thai Ministry of University Affairs for financial support.

References

- Qing Cai, J. B. a. S. W. Polymers For Advanced Technologies 2000, 11, 159-166.
- Srisard, M.; R. Molloy, N. M.; J. Siripitayanon, Sriyal, M. Polym. Int. 2001, 50, no. 8, 891-896.
- Khaled Mezghani, J. E. S. Journal of Polymer Science: Part B: Polymer Physics 1998, 36, 1005-1012.
- Jin Kon Kim, D.-J. P., Myung-Se Lee, Kyo Jin Ihn. Polymer 2001, 42, 7429-7441.
- S. Buchner, D. W. a. H. G. Z. Polymer 1989, 30, 480-448.

CONFERENCE PRESENTATIONS

in

**International Conference On Smart
Materials Smart/Intelligent Materials
and Nanotechnology**

held at

ลิขสิทธิ์มหาวิทยาลัยเชียงใหม่

Copyright © Imperial Mae Ping University

Chiang Mai, Thailand

All rights reserved

1st-3rd December 2004

**The International Conference
on Smart Materials**



SmartMat'04

Smart/Intelligent Materials and Nanotechnology



Celebrating the 40th anniversary of
Chiang Mai University

ลิขสิทธิ์มหาวิทยาลัยเชียงใหม่
Copyright © by Chiang Mai University
All rights reserved

1-3 December 2004

Imperial Mae Ping, Chiang Mai, Thailand

PP44: Investigation of the crystal Structure in Segmented Triblock L-lactide, ϵ -Caprolactone and Glycolide Terpolymer Fibres

Channuan, W¹, Siripitayananon, J¹, Molloy, R¹, Sriyai, M¹ and Mitchell, G: R.²

¹ Biomedical Polymers Technology Unit, Department of Chemistry, Faculty of Science, Chiang Mai University, Thailand 50200. E-mail : w.channuan@reading.ac.uk

² Polymer Science Centre and Department of Physics, University of Reading, Whiteknights, Reading RG6 6AF UK.

Segmented triblock terpolymers of L-lactide, ϵ -caprolactone and glycolide have the ability to biodegrade by simple hydrolysis in the human body. They therefore have the potential for use in biomedical applications such as absorbable surgical sutures. The particular terpolymer studied in this research project had an overall composition of L-lactide : ϵ -caprolactone : glycolide = 70 : 25 : 5 mol%. Monofilament fibres of the terpolymer were produced by melt spinning using a small-scale fibre extrusion apparatus. Under the processing conditions used, which involved rapid cooling, the as-spun fibres were obtained in an almost completely “quenched amorphous” state. Subsequent off-line hot-drawing and annealing steps were then employed to induce crystallisation and to build into the fibre the required degree of molecular orientation necessary to develop its mechanical properties. The dependence of these mechanical (tensile) properties on the processing conditions used was also studied, while X-ray diffraction (XRD) was used to determine molecular orientation and crystal structure. It was found that the crystal structure in the fibre after hot-drawing and annealing was predominantly that of the α -form of poly (L-lactide) and that it was this part of the matrix which was responsible for the fibre’s tensile strength.

ลิขสิทธิ์มหาวิทยาลัยเชียงใหม่

Copyright © by Chiang Mai University

All rights reserved



Investigation of the crystal Structure in Segmented Triblock L-lactide, ε-Caprolactone and Glycolide Terpolymer Fibres

Channuan, W., Siripitayanon, J., Molloy, R., and Sriyai, M.
Biomedical Polymers Technology Unit, Department of Chemistry, Faculty of Science
Chiang Mai University, Thailand 50200

Mitchell, G. R.
Polymer Science Centre, Department of Physics, University of Reading
Whiteknights, Reading RG6 6AF, UK.

ABSTRACT

Segmented triblock terpolymers of L-lactide, ε-caprolactone and glycolide have the ability to biodegrade by simple hydrolysis in the human body. They therefore have the potential for use in biomedical applications such as absorbable surgical sutures. The particular terpolymer studied in this research work had an overall composition of L-lactide : ε-caprolactone : glycolide = 70:25:5 mol %. Monofilament fibres of the terpolymer were produced by melt spinning using a small-scale fibre extrusion apparatus. Under the processing conditions used, which involved rapid cooling, the as-spun fibres were obtained in an almost completely "quenched amorphous" state. Subsequent off-line hot-drawing and annealing steps were then employed in order to induce crystallisation and to build into the fibre the required degree of molecular orientation necessary to develop its mechanical properties. The dependence of these mechanical (tensile) properties on the processing conditions used was also studied, while X-ray diffraction (XRD) was used to determine molecular orientation and crystal structure. It was found that the crystal structure in the fibre after hot-drawing and annealing was predominantly that of the α-form of poly(L-lactide) and that it was this part of the matrix which was responsible for the fibre's tensile strength.

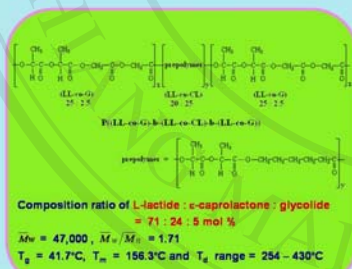
1. INTRODUCTION

Monofilament sutures have less affinity for bacteria and a smooth surface which are major advantages in exhibiting less tissue reaction and tissue drag. However, they tend to be quite stiff and difficult to handle which are disadvantages.

The new synthetic monofilament suture of particular interest in this work is a segmented triblock terpolymer of L-lactide (LL), ε-caprolactone (CL) and glycolide (G) with a composition of LL:CL:G = 70:25:5 mol %. One of our aims is to investigate the crystal structure in the fibre form.

2. EXPERIMENTAL METHODS

2.1 Materials



2.2 Fibre Processing

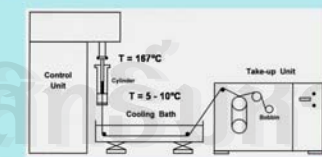


Fig 1 A small-scale melt spinning apparatus

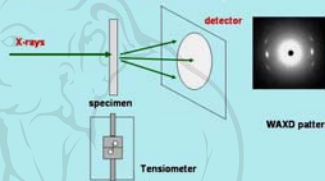
Off-line hot drawing

condition : Draw at Temp = 60°C
 Draw rate = 2500%/min
 Draw ratio = 5.9

Instruments for Fibre Characterization

Tensile Testing Machine : Study mechanical properties
 DSC : Degree of crystallinity

2.3 Wide-angle X-ray scattering



3. RESULTS

Table 1 Thermal and mechanical properties of the as-spun and drawn fibres

Fibre sample	Thermal properties				Mechanical properties		
	T _g (°C)	T _m (°C)	ΔH _m (J/g)	ΔH _m -LL (J/g)	Stress at break (MPa)	Young's modulus (MPa)	Strain at break (%)
As-spun fibre	42.7	154.3	13.2	23.6	8.4	195	347.7
Hot drawn fibre*	155.8	-	23.8	23.8	153	749	99

*The fibre was drawn to λ = 5.9 at 60°C with a draw rate of 2500 %/min

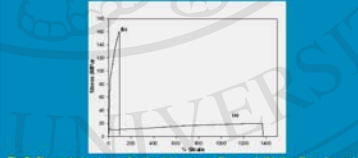


Fig 2 Stress-strain curves for the (a) as-spun fibre and (b) the fibre drawn to λ = 5.9 at 60°C with a draw rate of 2500 %/min.

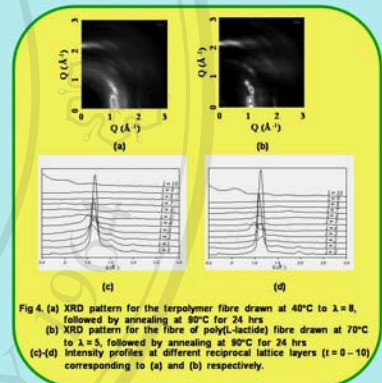


Fig 4. (a) XRD pattern for the terpolymer fibre drawn at 40°C to λ = 8, followed by annealing at 80°C for 24 hrs (b) XRD pattern for the fibre of poly(L-lactide) fibre drawn at 70°C to λ = 5, followed by annealing at 80°C for 24 hrs (c-d) Intensity profiles at different reciprocal lattice layers (l = 0-10) corresponding to (a) and (b) respectively.

4. CONCLUSION

The as-spun fibre obtained was largely amorphous with low strength. Hot drawing was then employed to enhance the fibre's strength, as a result of which it was found that, by drawing the as-spun fibre at 60°C at a rate of 2500 %/min to λ = 5.9, its strength increased to 8 times that of the as-spun fibre. From the DSC and XRD experiments, the results showed clearly that both crystallinity and molecular orientation were induced by hot-drawing and annealing and that increase were responsible for the fibre's strength. By comparing the XRD pattern of the drawn fibre with that of poly(L-lactide), it could be concluded that the terpolymer crystallized into the α-form of poly(L-lactide).

5. ACKNOWLEDGEMENTS

This work was supported by the National Metal and Materials Technology Center of Thailand (MTEC). One of us (W.C.) would also like to thank the Thai Ministry of University Affairs and the Graduate School and the Faculty of Science of Chiang Mai University for their financial support.

6. REFERENCES

- Bainmark, Y. and Molloy, R., Synthesis and characterization of Poly(L-lactide-co-ε-caprolactone) copolymers. Effects of stannous octoate initiator and diethylene glycol coinitiator concentrations, *Science Asia*, (in press).
- Toki, S., Sics, I., Ran, S., Liu, L., Hsiao, B. S., Murakami, S., Senoo, K. and Kohjiya, S., New insights into Structure Development in Natural Rubber during Uniaxial Deformation by In Situ Synchrotron X-ray Diffraction, *Macromolecules*, 2002, 35: 6578 - 6584.
- Medical DeviceLink, The effects of annealing conditions on the structure and properties of polypropylene fibers, Available at the website: <http://www.deviceink.com/20/6/2001>
- Hoogsteen, A. W., Postema, A. R., Pennings, A. J., Brinke, T. G. and Zugenmaier, P., Crystal Structure, Conformation, and Morphology of Solution-spun Poly(L-lactide) Fibres, *Macromolecules*, 1990, 23: 634-642.

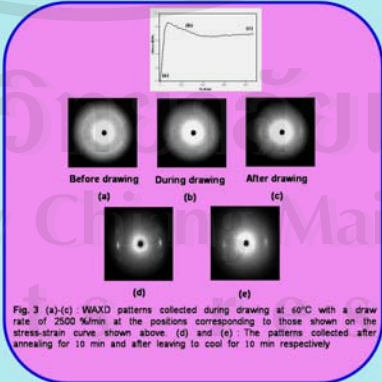


Fig 3 (a)-(c) WAXD patterns collected during drawing at 60°C with a draw rate of 2500 %/min at the positions corresponding to those shown on the stress-strain curve shown above. (d) and (e) The patterns collected after annealing for 10 min and after leaving to cool for 10 min respectively

CONFERENCE PRESENTATIONS

in

**The Fourth Thailand Materials Science
and Technology Conference**

held at

Thailand Science Park Convention

Center Thailand

31st March - 1st April 2006

NAC2006
NSTDA Annual Conference
Towards Sufficiency Economy with Science and Technology



Proceedings

The Fourth Thailand Materials Science and Technology Conference

■ March 31 – April 1, 2006 ■ Thailand Science Park

ลิขสิทธิ์มหาวิทยาลัยเชียงใหม่
Copyright © by Chiang Mai University
All rights reserved

organized by



NANO TEC



Structural Characterisation of Crystallisable Terpolymers of L-Lactide, ϵ -Caprolactone and Glycolide

Wasinee Channuan¹, Jintana Siripitayananon¹, Robert Molloy¹, Montira Sriyai¹
and
Geoffrey R. Mitchell²

¹Biomedical Polymers Technology Unit, Department of Chemistry, Faculty of Science, Chiang Mai University, Thailand 50200

Phone 0-5394-3341-5, Fax. 0-53892277, E-mail: jin-sc@chiangmai.ac.th

²Polymer Science Centre, Department of Physics, University of Reading, Whiteknights, Reading RG6 6AF, UK

Phone +44-118-378-8573, Fax. +44-118-975-0203, E-mail: g.r.mitchell@reading.ac.uk

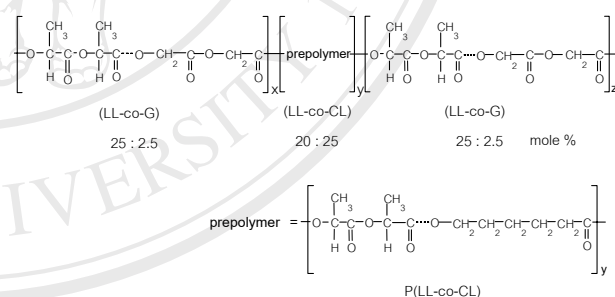
Abstract

Wide-angle and small-angle X-ray scattering together with optical microscopy were applied to study random and segmented triblock terpolymers prepared from L-lactide, ϵ -caprolactone and glycolide. In both cases, the overall fraction of lactide units is ~ 0.7 . By comparison of the WAXS patterns from hot drawn and annealed fibres of the terpolymers and the poly(L-lactide) homopolymer, we can show that the crystal structure is equivalent to the α phase of poly(L-lactide) for both, block and random terpolymers, although the fibres exhibit rather disordered structures. There are variations in the development of a two phase structure which reflect the differences in the chain architectures. There is an evidence that the random terpolymer includes non-lactide units into the crystal interfaces to achieve a well defined two-phase structure.

1. Introduction

Polyesters obtained on the basis of L-lactide (LL), ϵ -caprolactone (CL) and glycolide (G) are biocompatible and biodegradable and are widely used in biomedical applications including absorbable surgical sutures, controlled drug release and bone fixation⁽¹⁻⁴⁾. Their properties can be tailored to particular applications by adjusting the chemical configuration of the polymers in terms of the monomers used, their composition, thermal and mechanical treatments employed during the processing of the products. In many circumstances, properties depend largely upon the structure and the amount of crystallinity. Random co/terpolymers which contain 70% or more of LL and equivalent of sequence

lengths in block co/terpolymers may exhibit some crystallinity. Clearly, the local chain environment in a random co/terpolymers may differ greatly from that of a homopolymer system. This work focuses on determining the structural characteristics of the crystalline component of such co/terpolymers. The polyesters of particular interest in this work are random and segmented triblock terpolymers of LL, CL and G with an overall composition of LL : CL : G = 70 : 25 : 5 mol%. The molecular structure of the segmented triblock terpolymer is shown below.



Poly((L-lactide-co-glycolide)-b-(L-lactide-co- ϵ -caprolactone)-b-(L-lactide-co-glycolide))
 P((LL-co-G)-b-(LL-co-CL)-b-(LL-co-G))

These complex materials have potential used as absorbable monofilament sutures. The soft centre-block (prepolymer) provides good handling characteristics while the hard end blocks provide high strength. The strength provided by end blocks come from their ability to be crystallized. One of our aims is to investigate the crystal structure in fibres produced by melt-spinning, followed by hot-drawing and annealing under appropriate conditions. X-ray diffraction techniques and optical microscopy were employed to investigate the crystallization behaviour and structures of the two terpolymers.

2. Experimental

2.1 Materials and Characterization

A random terpolymer was synthesized via bulk polymerization using stannous octoate as a catalyst while a segmented triblock terpolymer with the same feed ratio of LL:CL:G = 70:25:5 mol % was synthesized via a 2-step reactions. The employed procedures were reported elsewhere⁽⁵⁾. Poly(L-lactide) was also synthesized from L-lactide by bulk polymerization for crystal structure comparison. The terpolymers and poly(L-lactide) were characterized by various analytical techniques: IR, ¹H-NMR, ¹³C-NMR, GPC, DSC and TG. The results are shown in Table 1

2.2 Wide-angle X-ray scattering (WAXS)

WAXS measurements were performed using a symmetrical transmission diffractometer, equipped with a graphite monochromator and pinhole collimation and a Cu K α source. Samples for scattering measurements were prepared by mounting lengths of fibres in a close packed parallel array. The X-ray scattering patterns for hot drawn and annealed fibres of the three polymers are shown in Fig. 1. The vertical or meridional axis is parallel to the fibre axis. All three fibres exhibit a high level of preferred orientation such that in all three patterns it is possible to identify the layer line structure associated with a single crystal type texture with rotational symmetry about the fibre axis. The basic features observed in Fig. 1 match those reported for the α phase of poly(L-lactide)⁽⁶⁾ both in terms of the peak position and intensity distributions. We have compared in more details the intensity distribution along each of different layer lines to those equivalent functions calculated for the α crystal structure and found excellent correspondence between the observed and calculated values confirming the presence of the α phase.

Table 1 Characterization of polymers

Polymer	LL:CL:G (mol%)	M _n	T _g (°C)	T _m (°C)	ΔH_m (°C)	T _d (J/g)
Poly(L-lactide)	-	12000	57.8	179.3	43.6	248-378
Random	76:19:4	33000	-33.3,34.8	143.9	7.6	252-390
Block	71:25:4	27000	41.7	156.3	25.2	254-430

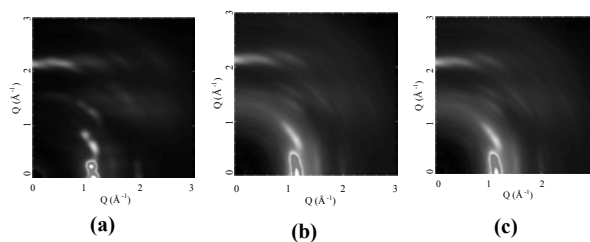


Fig. 1. X-ray scattering intensity maps for hot drawn and annealed fibres of (a) poly(L-lactide) (b) random terpolymer (c) block terpolymer. In each case the fibre axis is vertical.

2.3 Optical microscopy

The morphology of thin films of the polymers was investigated using a Swift-Bassett polarizing microscope equipped with a Mettler-Toledo programmable hot stage. Thin films were prepared by melting and pressing a small quantity of the polymer between two glass slides on a hot bar. Specimens were cooled at 20°C/min from the melt and then isothermally crystallized at the selected temperature (T_m -40°C). The crystalline nature of the terpolymers exhibited a strong, birefringent scattering texture (see Fig.2) with spherulite diameters of ~70-140 μ m. Optical microscopy studies during crystallisation reveal the linear spherulite growth rate. It is clear that the spherulite growth rate of the block copolymer is about twice that of the random terpolymer. The growth rate will be both a function of the composition and the sequence distribution as well as the molecular weight.

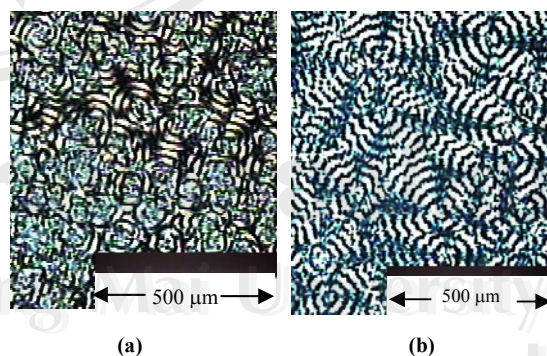


Fig. 2 Polarising optical micrographs of thin films at room temperature after crystallization at (a) 110°C random and (b) 120°C block terpolymer showing well defined spherulites.

2.4 Small-angle X-ray Scattering (SAXS)

SAXS experiments were performed on the fixed wavelength ($\lambda=1.4$ Å) beam-line 16.1 at the Daresbury Synchrotron Radiation Source (UK) using a beam ~

0.3mm diameter. Small-angle X-ray scattering (SAXS) data in the range $|Q| \sim 0.01$ to 0.12 \AA^{-1} were recorded using a 2-D RAPID detector with a data accumulation times of 10s. The SAXS patterns recorded for the annealed fibres show very strong and highly anisotropic scattering features as shown in Fig.3

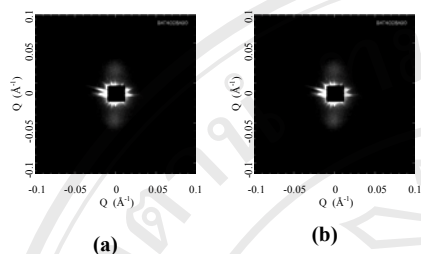


Fig. 3 Small-angle x-ray scattering patterns for the annealed fibres of (a) random terpolymer and (b) block terpolymer. In each case the fibre axis is vertical.

For the random terpolymer (Fig. 3 (a)), we see very sharp meridional peaks, at 0.038 \AA^{-1} , indicating a highly aligned two phase structure. The block copolymer fibre shows a similar pattern but the scattering is very much weaker with maxima at 0.031 \AA^{-1} . This indicates that the random terpolymer displays a highly developed lamellar stack type SAXS pattern, suggesting better defined crystals than in the block copolymer system. The SAXS patterns give long periods of the order of 160 \AA for the random terpolymer and 200 \AA for the block terpolymer.

3. Discussion and Conclusion

The methodology has been applied to two terpolymers with rather different architectures but both contain ~ 70 mole % of lactide units, although their positioning in the molecular chain differs. The WAXS and SAXS data indicates a detailed view of the multiple phase morphology. For both terpolymers, the crystallites are formed from the lactide units which is equivalent to the α phase of poly(L-lactide). The block terpolymer crystallizes more rapidly presumably due to the greater mobility of the end blocks.

It is also clear from SAXS that on the larger scale the two phase crystalline/non-crystalline structure is rather ill-defined in the block copolymer case. This attributes to the range of block lengths presented in the polymer

chains and the defect (i.e. non-inclusion) from the highly disordered central block containing very short sequences of both lactide and caprolactone. In contrast, the random copolymer exhibits a rather well defined two-phase structure which attributed to the greater extent that non-lactide units can be incorporated in to the interfaces of lamellar crystals to provide a smoother crystal face. This variation in the structure and dynamics of two materials with similar chemical composition but rather different architectures will be most helpful in the optimisation of these materials for use in biomedical applications.

In conclusion, random or block terpolymers exhibit a semi-crystalline structure in which the crystal component is essentially equivalent to the α crystal phase of poly(L-lactide). However, the random copolymer appears to have a very much better defined lamellar structure which we attribute to the ability of the random copolymer to incorporate minor levels of the other units in to the crystal interface in order to achieve a smoother crystal surface. This is particularly important for understanding the chemistry-structure-property relationships in these complex disordered polymer monofilaments with potential for use as absorbable sutures.

4. Acknowledgements

This work was supported by the National Metal and Materials Technology Centre (MTEC), Thailand and the Royal Society, UK, through the award of South-East Asia Fellowship to JS. We thank the Thai Ministry of University Affairs for financial support to WC.

5. References

- [1] Bezwada, R. S., et al. *Biomaterials* 1995; **16**: 1141-8.
- [2] Buntner, B., et al. *Journal of Controlled Release* 1998; **56**: 159-67.
- [3] Cai, Q., Bei, J. Z., and Wang, S. G. *Polymer(B)* 2002; **43**: 3585-91.
- [4] Dawes, E. and Rushton, N. *Biomaterials* 1997; **18**: 1615-23.
- [5] Channuan, W., Siripitayananon, J., Molloy R., Sriyai, M. and Mitchell, G. *Polymer* 2005; **46**: 6411-28.
- [6] Hoogsteen, W., et al. *Macromolecules* 1990; **23**: 634-42.

JOURNAL PUBLICATIONS

entitled

**The structure of crystallisable
copolymers of L-lactide, ϵ -caprolactone
and glycolide**

accepted on April 1st, 2005

ลิขสิทธิ์มหาวิทยาลัยเชียงใหม่

Copyright © by Chiang Mai University

All rights reserved

Polymer

(Available online 22 June 2005)

The structure of crystallisable copolymers of L-lactide, ϵ -caprolactone and glycolide

Wasinee Channuan^{a,b}, Jintana Siripitayananon^{a,b}, Robert Molloy^b,
Montira Sriyai^b, Fred J. Davis^a, Geoffrey R. Mitchell^{a,*}

^a*Polymer Science Centre, University of Reading, Reading RG6 6AF, UK*

^b*Department of Chemistry, Chiang Mai University, Chiang Mai 50200, Thailand*

Received 11 December 2004; received in revised form 29 March 2005; accepted 1 April 2005

Available online 22 June 2005

Abstract

We apply a new X-ray scattering approach to the study of melt-spun filaments of tri-block and random terpolymers prepared from lactide, caprolactone and glycolide. Both terpolymers contain random sequences, in both cases the overall fraction of lactide units is ~ 0.7 and ^{13}C and ^1H NMR shows the lactide sequence length to be ~ 9 – 10 . A novel representation of the X-ray fibre pattern as series of spherical harmonic functions considerably facilitates the comparison of the scattering from the minority crystalline phase with hot drawn fibres prepared from the poly(L-lactide) homopolymer. Although the fibres exhibit rather disordered structures we show that the crystal structure is equivalent to that displayed by poly(L-lactide) for both the block and random terpolymers. There are variations in the development of a two-phase structure which reflect the differences in the chain architectures. There is evidence that the random terpolymer includes non-lactide units in to the crystal interfaces to achieve a well defined two-phase structure.

© 2005 Published by Elsevier Ltd.

Keywords: X-ray scattering; Structure; Orientation

1. Introduction

Copolymers of L-lactide with units such as ϵ -caprolactone and glycolide have been proposed and used in a wide variety of biomedical applications including absorbable monofilaments sutures [1], controlled drug release [2–4] and bone fixation [5–8]. The properties can be tailored to particular applications by adjusting the chemical configuration of the polymers in terms of the monomers used and their composition together with the thermal and mechanical treatments employed during the processing of the products. In many circumstances, the key to the definition of the properties is the control of the crystallisation of the lactide units within the copolymer structure. Homopolymers of L-lactide exhibit a number of

crystalline phases whose structures have been determined from X-ray patterns of highly aligned fibres. The particular phase displayed appears to depend on the processing route of the fibres, the most common structure is the α phase which exhibits a $-10/3$ helical chain conformation [9–11] but hot fibre drawing may lead to the formation of the β phase which is based on a $3/1$ helix [12]. As with many helical structures, interactions between neighbouring chains play an important part in stabilising particular structures and detailed work by Puiggali et al. has identified specific frustrated packing schemes which arise from differing parallel and antiparallel arrangements of neighbouring chains [12,13]. Random copolymers which contain 70 mol% or more of lactide and equivalent sequence lengths in block copolymers may exhibit some crystallinity. Clearly the local chain environment in a random copolymer may differ greatly from that in a homopolymer system. This contribution focuses on determining the structural characteristics of the crystalline component of such copolymers. These are complex materials with a number of components and phases. Analysis of the X-ray diffraction data is not all straightforward even from highly aligned fibres and we have

* Corresponding author. Tel.: +44 118 378 8573; fax: +44 118 975 0203.

E-mail address: g.r.mitchell@reading.ac.uk (G.R. Mitchell).

developed a new approach which facilitates the comparison of data from partially oriented, poorly ordered systems. In particular we contrast a random terpolymer and a tri-block terpolymer with similar overall compositions but with different distributions of monomer units within the polymer chain and explore if the 10/3 helical chain conformation of crystalline poly(L-lactide) [14], is replicated in these copolymers.

2. Materials

L-lactide (LL) and glycolide (G) were synthesized using established procedures from L-lactic acid and glycolic acid (purchased from CARLO ERBA Reagenti) and purified by re-crystallization from ethyl acetate to a purity of 99.8 mol% determined by DSC. ϵ -Caprolactone (CL) was purchased from Aldrich Chemicals and purified by distillation under reduced pressure and stored over molecular sieves. Stannous octoate was purchased from Sigma Chemical Co. Ethyl acetate and diethylene glycol were distilled before use.

Poly(L-lactide) was synthesized by bulk polymerization of L-lactide using stannous octoate as a catalyst at 140 °C for 72 h. A random copolymer, P(LL-ran-CL-ran-G) was prepared by simultaneous addition of three monomers with a feed ratio of LL:CL:G=70:25:5 (mol%) into a reactor in the presence of 0.04% (w/w) stannous octoate at 140 °C for 18 h initially under a dry nitrogen atmosphere and finally under reduced pressure [15,16].

A block copolymer P(LL-ran-G)-block-P(LL-ran-CL)-block-P(LL-ran-G) (Fig. 1) was prepared using a two stage approach. First, a soft centre-block containing a random distribution of LL and CL units was prepared through melt phase polymerisation at 140 °C for 10 h with stannous octoate as a catalyst and diethylene glycol as an initiator. This 2 hydroxy-terminated (P(LL-ran-CL)diol) was used as

a macro initiator for the subsequent polymerisation of the end blocks containing a random distribution of LL and G at 150 °C for 10 h [4,17]. Homopolymerization of the LL is inhibited by the consumption of the stannous octoate during the first phase. The soft centre-block was prepared using a charge of 4:5 in terms of LL and CL. The two hard end-blocks were prepared using a charge of 10:1 in term of LL and G.

In all cases the polymers were vacuum-dried at 100 °C for 24 h to remove any unreacted monomers. Typically, polymer yields of 98 w/w% were obtained.

3. Polymer characterization

The chemical compositions of the terpolymers were determined from the peak area integrations in the ¹H NMR spectra, the peak at δ =5.0–5.3 ppm corresponding to the methine hydrogen (CH) in the LL units, at δ =4.0–4.2 ppm corresponding to methylene hydrogen (CH₂) attached to the oxygen in a repeating CL unit and the area of the peak at δ =4.5–4.9 corresponding to methylene hydrogen in the G units. Expanded sections of the proton NMR are shown in Fig. 2 and the compositions of the terpolymers obtained are shown in Table 1. The compositions largely reflect the feedstock although in the case of the lactidyl units an excess was observed in the block polymer with an observed composition of 76 mol% compared with an expected composition of 70 mol%.

Table 1 also shows the number-average molecular weight (M_n), the polydispersity index (M_w/M_n) and the intrinsic viscosity, $[\eta]$ for the polymers prepared in this work. The molecular weight data for the terpolymers were determined by gel permeation chromatography (GPC) in tetrahydrofuran using polystyrene standards. The intrinsic viscosities, $[\eta]$, of the poly(L-lactide) were measured with Ubbelohde viscometer in chloroform at 30 °C and used to

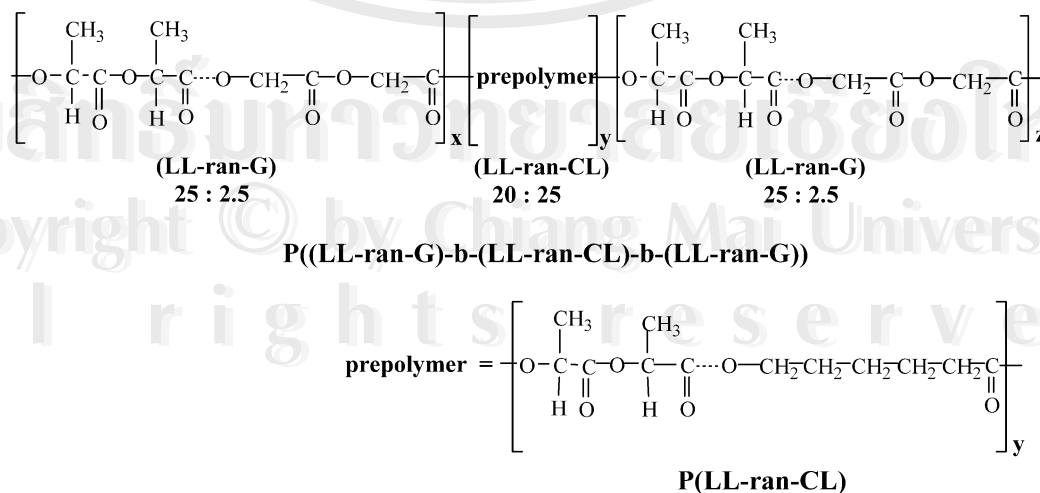


Fig. 1. A schematic of the chemical configuration of the block terpolymer used in this work showing the composition of both the prepolymer or macro initiator and the terminal blocks.

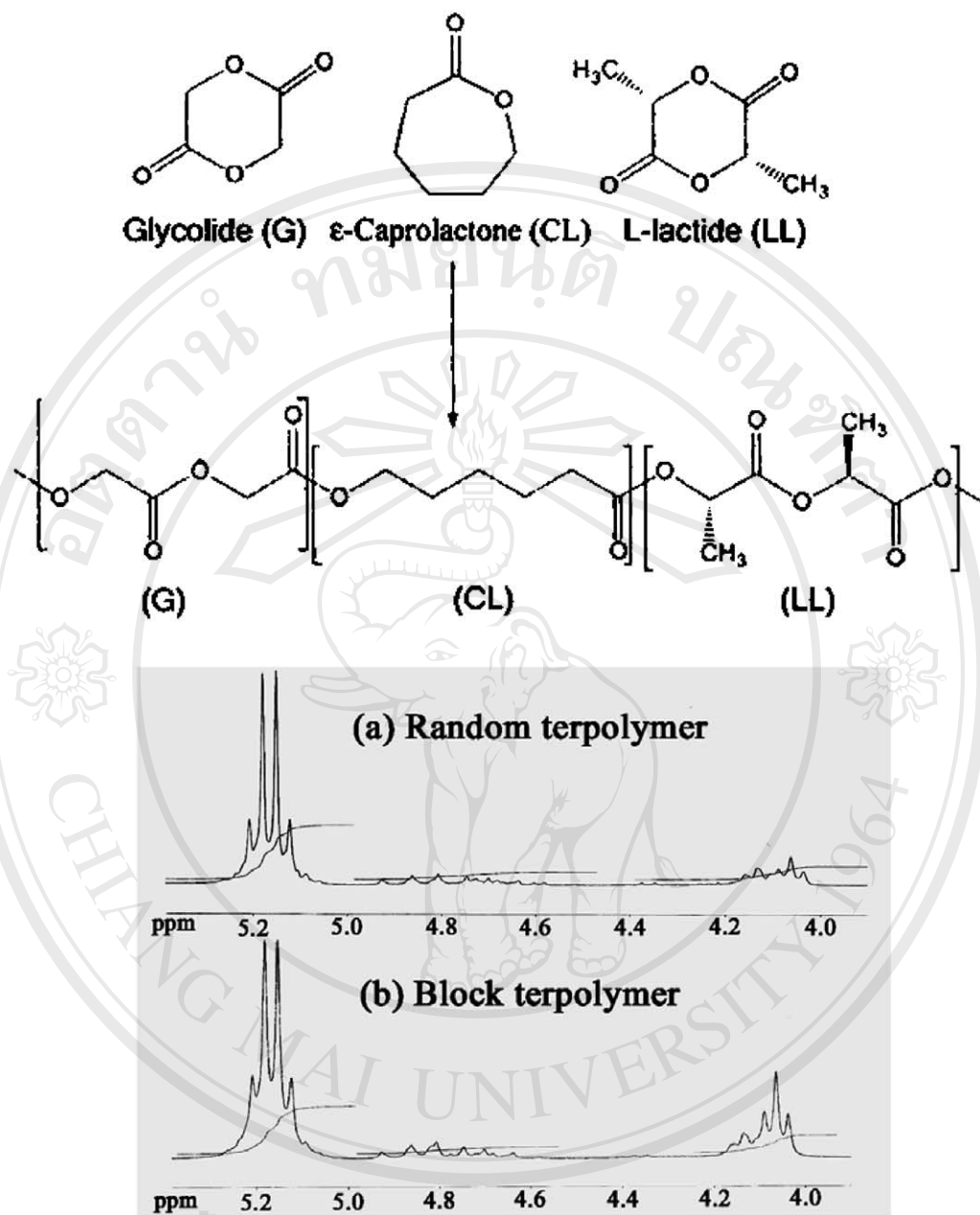


Fig. 2. A schematic of the monomers and the resultant polymer sequences and the nmr spectra used to determine the distribution of carbonyl groups in each section.

Table 1
Characterisation of polymers

Polymer	GPC		[η] (dl/g)	¹ H NMR monomer composition LL:CL:G (mol%)
	M_n	M_w/M_n		
Poly(L-lactide)	12,000	–	0.45	–
Random terpolymer	33,000	1.85	1.27	76:19:4
Block terpolymer	27,000	1.71	0.98	71:25:4

estimate M_n using the calibration equation proposed by Nijenhuis et al. [18].

$$[\eta] = 3.25 \times 10^{-4} M_n^{0.77} \text{ dLg}^{-1}$$

The properties of the materials produced, in particular the phase behaviour, are influenced by the length of sequences of individual monomer units [19–21]. In the polymers considered here, these structural characteristics can be determined by NMR. Both ¹³C and ¹H NMR can be used to this end [22]. The polymers under investigation are terpolymers produced by the ring-opening polymerisation of the three monomers shown in Fig. 2. Consideration of the monomers reveals that the polymerisation reaction will

inherently produce twin sequences of the lactidyl (L) and glycolidyl (G) units; with the caproyl (Cap) groups appearing as single units. However, previous studies suggest that the system will be more complex than this with transesterification producing ‘unexpected’ sequences such as CapLCap [23].

The assignment of individual sequences from the NMR spectra used here is based on the work of Dobrzynski [22], which is in turn based on a body of work concerning chain sequences of the various combinations of two of the three monomer units. For example, copolymers of L-lactide and ϵ -caprolactone have been analysed [24,25]. The analysis makes use of the carbonyl signals from the ester units; for sequences containing only caprolactone, a singlet is observed at 173.5, while for the lactate-based system the homopolymer shows a signal at 169.6 ppm.¹ The situation is made more complex for the lactidyl and glycolidyl units by the fact that once the symmetry is reduced by the presence of co monomer units, the two carbonyls in the repeat unit exhibit different chemical shifts. The presence of transesterification in the polymer can be detected by the presence of isolated lactidyl or glycolidyl units [25].

The analysis uses the triad sequences to determine the average block length of the individual components as given in Eq. (1) (where X may be for example one half of the lactidyl unit and Z may be either Caprolactyl or glycolidyl).² Where the technique is sensitive to longer sequences, and this is particularly the case for ¹³C NMR, the triad sequences need to be calculated from (for example pentad) sequences. Thus, for example, the CapLLCap sequence contains 1 CapLL and 1 LLCap triad and must be weighted accordingly [26]. We have used both ¹³C and ¹H NMR data to analyse the sequence distribution and the data obtained are shown in Table 2

$$l_{XX} = \frac{1}{2} \frac{XXX + ZXX + XXZ + ZXZ}{ZXZ + \frac{1}{2}(XXZ + ZXX)} \quad (1)$$

The sequence lengths appear to largely reflect the distributions expected for random copolymers with more or less equal reactivities. The main differences in the NMR between the so-called block and random samples is that the block terpolymer sample clearly shows a much higher proportion of the CapCapCap triad than is observed for the random sample with 60% for the block and 37% for the random. This of course is entirely in line with expectations based on the method used to synthesize the materials. In particular, since in the block copolymer the caprolactone is restricted to one of the blocks, the overall equivalent concentration appears contiguously in longer sequence lengths than broken up as in the random terpolymer. No

Table 2
Sequence lengths for copolymer system

Terpolymer	Sequence length		
	l_{LL}	l_{GG}	l_{Cap}
Block ¹ H	8.1	0.79	3.8
Block ¹³ C	7.5	^a	4.0
Random ¹ H	9.0	0.85	2.3
Random ¹³ C	9.8	^a	2.2

^a Unable to assign peaks unambiguously hence no value available.

conclusion could be drawn from the glycidyl units from the ¹³C NMR because of difficulties assigning the NMR peaks unambiguously, however, the data from the ¹H NMR is included. The only other particularly noticeable feature is that a signal which can be assigned to a CapLCap triad is observed for the block sample, but not for the random sample. It is the presence of this unit that may in part explain the lower average lactidyl sequence length for the block polymer. Apart from this peak, there is some evidence for anomalous CapLCap and GLG sequences; however, these are not a major feature of the NMR. Thus it would seem transesterification has little effect on the lactidyl units. The glycidyl units in contrast seem rather more effected by this process and a peak at 4.81 ppm in the ¹H NMR which can be related to the presence of isolated glycidyl units is the most prominent in this region of the spectrum. As a consequence, the average sequence length for the glycidyl units is less than 1. One final feature of the ¹H NMR which is worthy of note, is that while most of the spectrum is comparable to that given by Dobrzynski [22], the caprolactone region differs substantially. In particular the CapCap sequences are present in substantially higher concentrations than the GCap and LCap sequences; in the NMR presented by Dobrzynski for a polymer of similar composition, the situation is reversed. This presumably relates to the different method of polymerisation used.

In the case of the block copolymer, there are two types of lactidyl sequences. The first are those involving the copolymerisation of lactide with caprolactone to form the macro initiator or middle block and the second are those located in the end blocks copolymerised with glycolide. It is not possible to differentiate in the NMR spectra between these two types of sequences and as a consequence the estimate of the average sequence length involves an average over the two types. If we assume that for the centre block, the units are arranged randomly according to composition alone we can estimate that the sequence length of the lactide units in the two outer blocks is ~ 10 . As the molecular weight data were obtained from GPC measurements calibrated with polystyrene standards, there will always be some doubt as to the absolute values. However, if we combine the GPC and NMR data, we can develop a picture of the block copolymer with the middle block containing some 80–90 and LL units, while the end blocks each contain some 50–60 units which are largely LL. The CL

¹ The chemical shifts are quoted from the appropriate publications, these values may vary slightly with for example change of solvent; the relative positions should remain unchanged.

² The factor of 1/2 is only suitable for the double monomer units.

units are restricted to this central block. Within the end blocks, the LL units exhibit an average sequence length of ~ 10 , separated by glycolide units. In contrast, the random terpolymer contains LL sequences of some 9 units but which are distributed throughout the chain separated by either glycolide units or short sequences of caprolactone. The caprolactone units are distributed throughout the chain.

4. Experimental

4.1. Wide-angle X-ray scattering

Wide-angle X-ray scattering measurements were made using a symmetrical transmission diffractometer equipped with a graphite monochromator and pinhole collimation and a Cu K-source. The intensity values from isotropic samples were obtained as a function of $|Q|$ over the range $0.2\text{--}6\text{ \AA}^{-1}$ in steps of 0.02 \AA^{-1} where $|Q|=4\pi\sin\theta/\lambda$, 2θ is the scattering angle and λ is the incident X-ray wavelength. Data for anisotropic samples were obtained both as a function of $|Q|$ over the range $0.2\text{--}6\text{ \AA}^{-1}$ in steps of 0.02 \AA^{-1} and of α , over the range $0\text{--}90^\circ$ in steps of 2° . α is the angle between the symmetry axis of the sample and the scattering vector Q . The scattering data were corrected for the effects of absorption, polarisation, multiple and incoherent scattering and scaled to absolute units using standard procedures [27]. Samples for scattering measurements were prepared by mounting lengths of fibres in a close packed parallel array. Typically the X-ray beam samples 2–3 fibres.

The rate of crystallization and the final fraction of crystallinity in each polymer were determined using a 2-circle X-ray diffractometer equipped with a graphite monochromator, pinhole collimation and a Cu-source. The diffractometer contained a heating stage for mounting 2 mm diameter Lindemann glass capillaries which allowed the temperature to be controlled within $\pm 1^\circ\text{C}$. Samples were melted in a Lindemann glass capillary and quenched rapidly using iced water. Subsequent X-ray scattering measurements showed these samples to be completely non-crystalline. The hot-stage used for the X-ray scattering measurements were preheated to the selected isothermal crystallisation temperature and the capillary rapidly lowered in to the hot-stage. At this stage, the wide-angle X-ray scattering data were collected to follow the nature of the crystallisation process. A series of short scans centered on $|Q|=1.18\text{ \AA}^{-1}$ were taken on a continuous basis to monitor the development of a crystalline structure and the intensity recorded as a function of time. After the crystallization process was completed, the scattered intensities were recorded as a function of $|Q|$ from 0.2 to 6.0 \AA^{-1} in step of $\Delta Q=0.02\text{ \AA}^{-1}$. Estimates of the crystallinity were made by separating the crystalline and non-crystalline components of the wide-angle X-ray scattering data using standard non-linear least squares peak-fitting procedures in

the region $|Q|$ from 0.5 to 2.0 \AA^{-1} . The fraction of crystallinity was calculated from the ratio of the $|Q|^2$ weighted integral of the crystalline peaks to the equivalent integral for the total scattering. Such an approach yields the fraction of crystallinity as a function of time, which enabled the rate of conversion or crystallisation rate to be evaluated for each particular isothermal crystallisation temperature.

4.2. Small-angle X-ray scattering

Small-angle X-ray scattering experiments were performed on the fixed wavelength ($\lambda=1.4\text{ \AA}$) beam-line 16.1 at the Daresbury synchrotron radiation source (UK) using a beam $\sim 0.3\text{ mm}$ diameter. Small-angle X-ray scattering (SAXS) data in the range $|Q|\sim 0.01\text{--}0.12\text{ \AA}^{-1}$ were recorded using a 2-D RAPID detector with a data accumulation times of 10 s. The intensity data were normalised to the incident beam using the values obtained from an ionisation chamber prior to the sample. The SAXS detector was calibrated in terms of geometry using the scattering from a collagen sample obtained from a rat tail tendon mounted in place of the fibre samples.

4.3. Optical microscopy

The morphology of thin films of the polymers was investigated using a Swift-Bassett polarizing microscope equipped with a Mettler-Toledo programmable hot stage. The thin films were prepared by melting and pressing a small quantity of the polymer between two glass slides on a hot bar. Specimens were cooled at $20^\circ\text{C}/\text{min}$ from the melt and then, isothermally crystallized at the selected temperature.

4.4. Thermal analysis

The glass transition temperature (T_g) and the melting behaviour of the polymers were measured by differential scanning calorimetry (DSC, Perkin–Elmer 2). The instrument was calibrated with indium, dodecane and ammonium sulfate. Each sample of $\sim 5\text{ mg}$ was heated at a rate of $20^\circ\text{C}/\text{min}$ in the range of $-70\text{--}180^\circ\text{C}$ in all cases, except for Poly(L-lactide) for which a scan rate of $10^\circ\text{C}/\text{min}$ and a range of $20\text{--}200^\circ\text{C}$ was employed. Thermal degradation data were obtained by TGA7 thermo-gravimetric analyzer at a heat rate of $20^\circ\text{C}/\text{min}$ and heat from $50\text{ to }600^\circ\text{C}$ under dry nitrogen.

4.5. Fibre drawing

Initial monofilaments were prepared using a small-scale melt spinning apparatus employing a batch size of 5–10 g. The processing parameters used to prepare monofilaments of the random terpolymer, the block terpolymer and poly(L-lactide) monofilaments are shown in Table 3. Using this approach monofilaments with a

Table 3
Conditions used for monofilament preparation

Polymer	Extrusion chamber temperature (°C)	Extrusion rate (mm/min)	Cooling bath (10–15 °C) used	Windup speed (mm/min)
Random terpolymer	155	0.07	Yes	0.5
Block terpolymer	167	0.10	Yes	1.0
Poly(L-lactide)	195	0.05	No	3.0

smooth surface were successfully produced with diameters of 0.4–0.6 mm. These as-spun fibres were then vacuum dried and kept in a vacuum dessicator until required.

The as-spun monofilaments were subjected to a variety of coupled mechanical and thermal treatments in order to produce samples with highly oriented crystalline structures. These conditions are shown in Table 4. The annealed samples were used for the initial structural analysis. The mechanical properties of the unannealed filaments are more typical of the requirements for absorbable monofilament sutures [2].

5. Crystallisation from a quiescent melt

The wide-angle X-ray scattering curves (Fig. 3) measured at room temperature for samples of the three polymers which have been cooled from the melt exhibit both sharp and broad peaks typical of a semi-crystalline polymer. The three patterns show considerable similarity. The data for poly(L-lactide) has substantial peaks at $|Q| \sim 1.12, 1.28, 1.98$ and 2.2 \AA^{-1} . The random terpolymer sample shows peaks at $|Q| \sim 1.16, 1.32$ and 2.14 \AA^{-1} while the block terpolymer samples sharp peaks at $|Q| \sim 1.14, 1.30,$ and 2.14 \AA^{-1} . It is not surprising that the sharp peaks in the patterns of the two terpolymers are somewhat broader and relatively less intense than the similarly positioned peaks for the poly(L-lactide).

The crystalline nature of the two terpolymers was further supported by the observation that samples cooled from the melt exhibited a strong, birefringent scattering texture, albeit with no distinctive features on scale accessible in an optical microscope. However, samples crystallised isothermally at temperatures close to the melting point revealed a

distinctive banded spherulitic structure (Fig. 4) with spherulite diameters of $\sim 70\text{--}140 \mu\text{m}$. Poly(L-lactide) crystallised under equivalent conditions exhibited non-banded spherulites. The observation of the banded spherulites in the case of the terpolymers and not in the homopolymer serves to underline the basic precepts of the banded spherulite model proposed by Bassett et al. [28]. Optical microscopy studies during crystallisation reveal a typical linear spherulite growth rate. It was clear that the spherulite growth rate of the block copolymer is about twice that of the random terpolymer at the equivalent quench step below the melting point. The growth rate will be both a function of the composition and the sequence distribution as well as the molecular weight. As the homopolymer studied here has a different molecular weight to both block and random terpolymers, we have plotted in Fig. 5 the radial growth rates observed at a temperature corresponding to a constant degree of under cooling of $(T_m - 40)^\circ\text{C}$ for the three polymers produced in this study as a function of molecular weight along with some additional data for poly(L-lactide)s of different molecular weights taken from the literature [29–31]. The growth rates for the two terpolymers fall substantially below the fitted line for the poly(L-lactide). Clearly the chemical microstructure of the terpolymers has greatly reduced both growth rates with the random terpolymer being the most affected.

The results of the DSC studies of the three polymers are shown in Table 5. The glass transition temperature and melting point for the poly(L-lactide) are similarly to those reported in the literature, for example [31]. Equivalent DSC studies of the block and random terpolymer samples reveal somewhat lower glass transition and melting temperatures as is expected for random copolymers. We have calculated the glass transition and the melting temperature using the Fox and Flory equations [20,32] using the values of the equilibrium melting temperature and enthalpy change for the equivalent homopolymers [33,34] and these are recorded for the random terpolymer in Table 5. The correspondence between experimental and predicted values underpins the random nature of the terpolymer. Thermo gravimetric studies showed that the onset of significant degradation did not take place until $\sim 250^\circ\text{C}$.

In order to investigate the crystallisation behaviour of the two terpolymers in more detail, we carried out isothermal crystallisations at a series of temperatures using wide-angle X-ray scattering techniques as described earlier to evaluate

Table 4
Drawing conditions for the post-spinning treatment

Polymer	Drawing temperature (°C)	Draw rate (%/min)	Draw ratio	Annealing temperature (°C)	Annealing time (h)
Random terpolymer	40	300	4.0	–	0
Random terpolymer	40	700	8.0	80	24
Block terpolymer	40	1000	4.5	–	0
Block terpolymer	40	1000	8.0	90	1
Poly(L-lactide)	70	2400	5	90	24

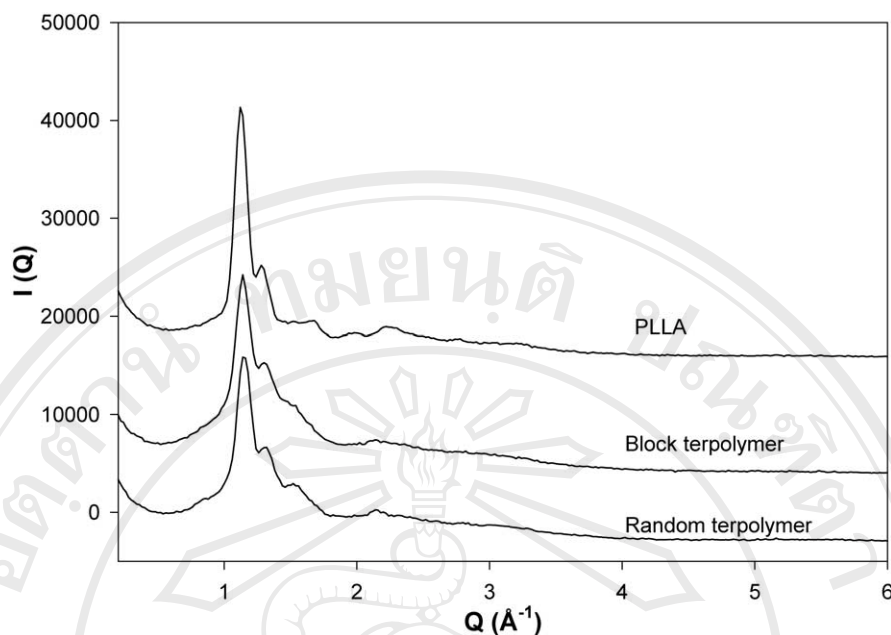


Fig. 3. Plots of the experimental wide-angle X-ray scattering intensity $I(Q)$ recorded for samples of poly(L-lactide) (PLLA), random terpolymer and block terpolymer crystallised from a quiescent melt.

the level of crystallinity. We used the intensity of the sharp diffraction feature at $|Q| \sim 1.2 \text{ \AA}^{-1}$ recorded as a function of time to evaluate the crystallization rate or conversion rate at each temperature. Fig. 6(a) shows a plot of the rate of crystallisation for a range of isothermal crystallisation temperatures for the two terpolymers. These data reveals the typical bell-shaped curve with a maximum crystallisation rate for the random terpolymer at $\sim 90 \text{ }^\circ\text{C}$ and for the block terpolymer at $100 \text{ }^\circ\text{C}$. We have also plotted (Fig. 6(b)) the plateau level of crystallinity observed at the end of each crystallisation sequence. These measurements were made by separating the crystalline and non-crystalline components of the wide-angle X-ray scattering data using standard peak-fitting procedures as described earlier. Over the temperature range $50\text{--}120 \text{ }^\circ\text{C}$ the fraction of crystallinity

lies in the range of 15–20%. There is a suggestion that the random terpolymer exhibits a slightly higher level of crystallinity at lower temperatures.

6. Structure of hot drawn fibres

6.1. Fibre patterns and related data

In order to obtain more detail on the structure of the crystalline components in the two terpolymers we have obtained maps of the X-ray scattering data for hot drawn fibres of the three polymers and these are shown in Fig. 7. Although these have the superficial appearance of traditional X-ray fibre patterns, it is emphasised that these

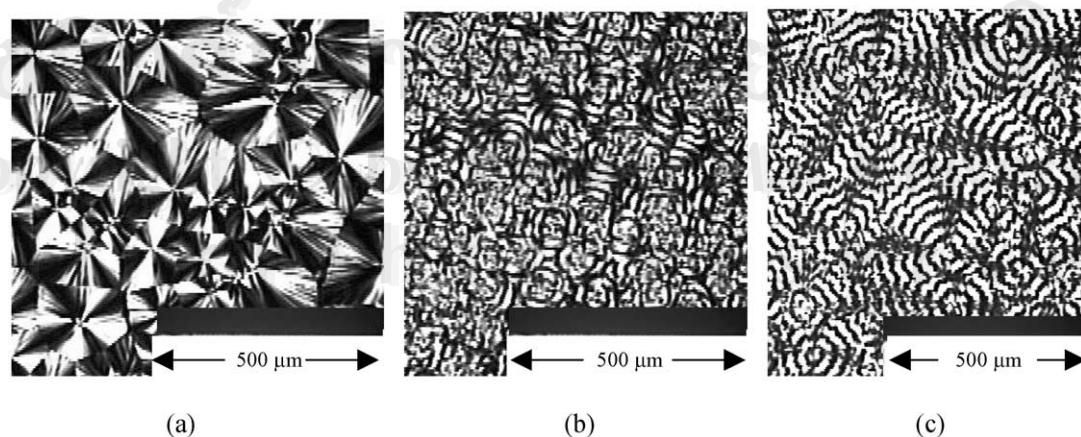


Fig. 4. Polarising optical micrographs of thin films at room temperature after crystallisation at (a) $130 \text{ }^\circ\text{C}$, poly(L-lactide); (b) $110 \text{ }^\circ\text{C}$ random terpolymer and (c) $120 \text{ }^\circ\text{C}$ block terpolymer showing well defined spherulites which for (b) and (c) are strongly banded.

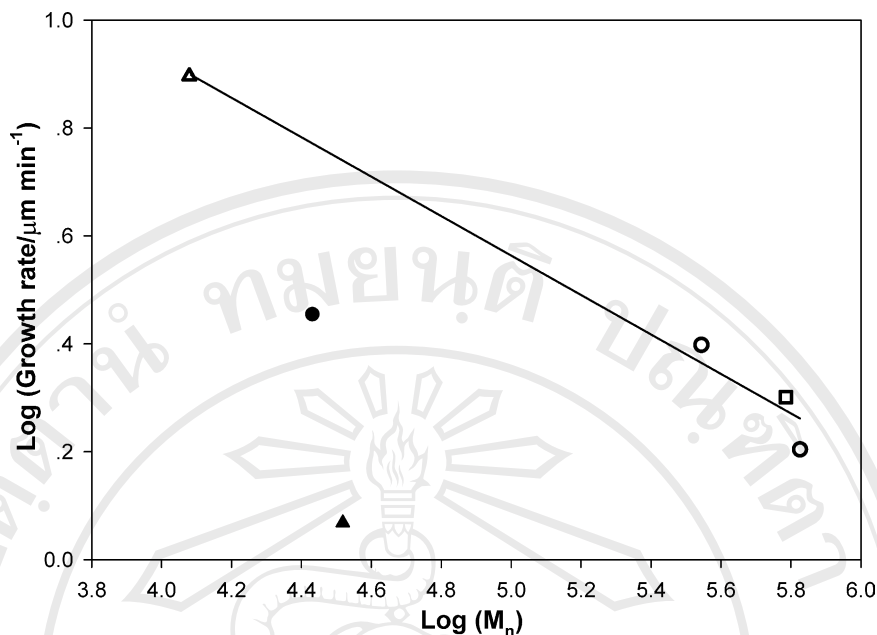


Fig. 5. A plot of the radial growth rate of spherulites against the molecular weight (M_n) for ▲ random terpolymer, ● block terpolymer and △ poly(L-lactide) prepared in this work together with data for poly(L-lactide) taken from Ref. [30] (○) and Ref. [31] (□). The growth rates were measured at a constant degree of undercooling of ~ 40 °C. The line represents a fit to the poly(L-lactide) data on the basis of a simple power law relationship between growth rate and molecular weight.

are true undistorted reciprocal space maps of the scattered intensity. The vertical or meridional axis is a parallel to the fibre axis and is the axis of cylindrical symmetry. The horizontal or equatorial axis lies normal to the fibre axis. The point marked 0,0 would correspond to the central part of a traditional fibre pattern. The accompanying sections show the intensity along the meridional and equatorial sections. All three fibres exhibit a high level of preferred orientation such that in all three patterns it is possible to identify the layer line structure associated with a single crystal type texture with rotational symmetry about the fibre axis. There is clearly considerable similarity between the patterns.

The poly(L-lactide) pattern has peaks in equatorial section at $|Q| \sim 1.14, 1.46$ and 1.96 \AA^{-1} . On the meridional section there is a prominent peak at $|Q| \sim 2.14 \text{ \AA}^{-1}$. Three crystal phases have been observed for poly(L-lactide). The most common form exhibits an orthorhombic unit-cell ($a = 10.7 \text{ \AA}$, $b = 6.45 \text{ \AA}$ and $c = 27.8 \text{ \AA}$) in which the molecules

adopt a 10/3 helical conformation. Hoogsteens et al. found that by adjusting the fibre processing conditions, two other structures may be observed [10]. The so-called beta structure also exhibits an orthorhombic unit cell ($a = 10.31 \text{ \AA}$, $b = 18.21 \text{ \AA}$ and $c = 9.00 \text{ \AA}$) in which the molecules possess a 3/1 helical conformation [10]. The third possibility is the γ phase which is formed by the frustrated packing of three fold helices within an orthorhombic unit cell with $a = b = 10.52 \text{ \AA}$ and $c = 8.8 \text{ \AA}$. The basic features observed in Fig. 7(a) match those reported for the alpha phase of poly(L-lactide) [10] both in terms of the position and intensity distributions of the meridional (c repeat) and the $hk0$ equatorial reflections.

In Fig. 8 we have plotted horizontal sections of the data shown in Fig. 7(a) taken at regular intervals of $2\pi/c$ corresponding to the so-called layer lines on which scattering intensity is confined for a uniaxial fibre. We observed, as expected for the α phase, that the first layer line with intensity peak on the meridian corresponds to the 10th

Table 5
DSC data

Polymer	DSC					TGA
	T_g (°C)	T_g Calc ^a (°C)	T_m ^b (°C)	T_m Calc ^c (°C)	ΔH_m (J/g)	T_d range (°C)
Poly(L-lactide)	57.8		179.3		43.6	248–378
Random terpolymer	–33.3, 34.8	35.4	143.9	143.5	7.65	252–390
Block terpolymer	41.7		156.3		25.2	254–430

^a Calculated using the Fox equation [32].

^b T_m is taken at the maximum of the endotherm.

^c Calculated using the Flory equation [20] and data from Refs. [33,34].

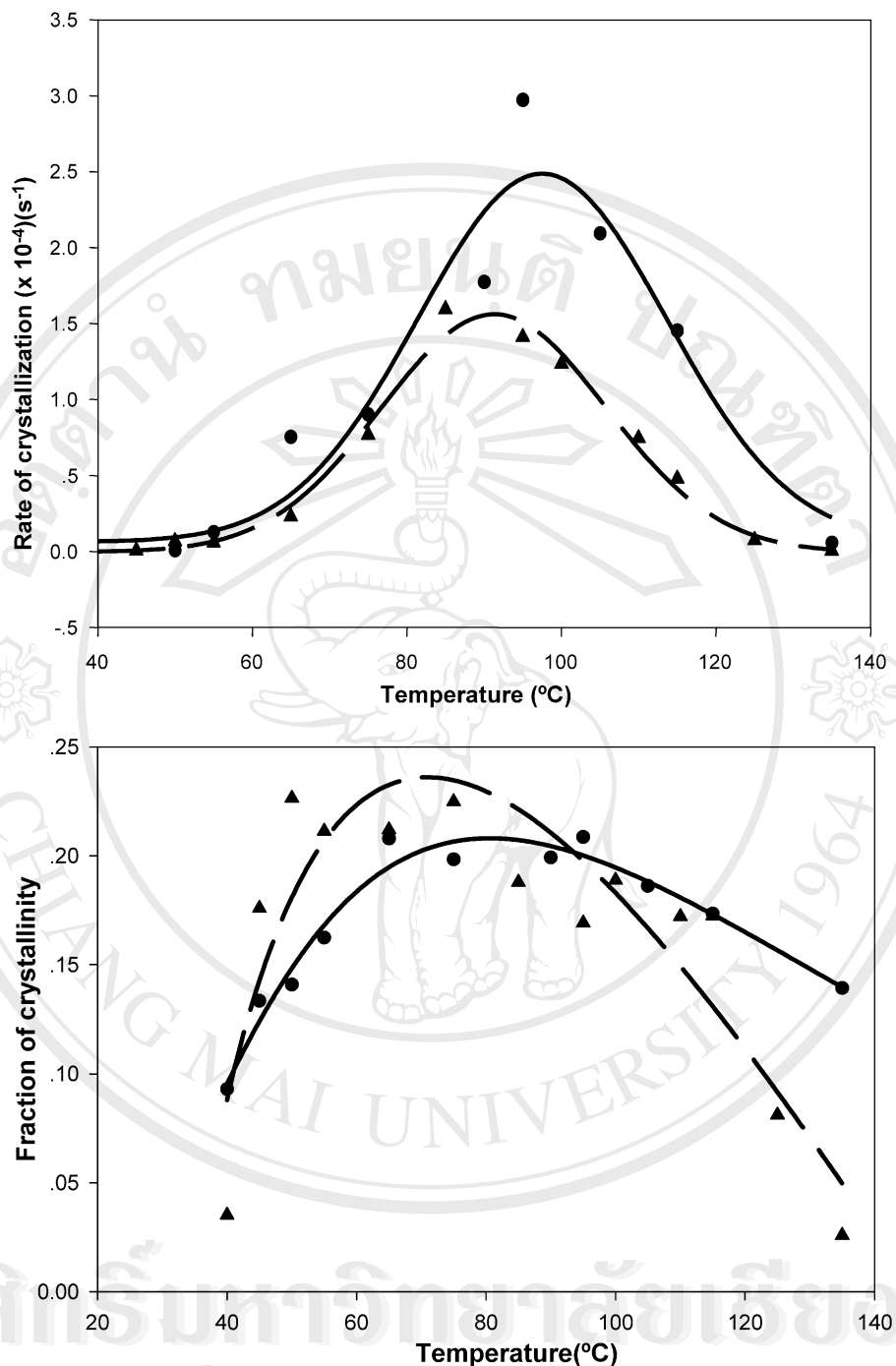


Fig. 6. (a) A plot of the rate of crystallisation as a function of the isothermal crystallisation temperature for the random terpolymer (▲, dashed-line) and the block copolymer (●, full line) derived from time-resolving wide-angle X-ray scattering data; (b) a plot of the final fraction of crystallinity in samples of the random terpolymer (▲, dashed-line) and the block copolymer (●, full line) as a function of the isothermal crystallisation temperature.

layer. We have compared the intensity distribution along each of these layer lines which the equivalent functions calculated for the α crystal structure, for example Fig. 8 in Ref. [14]. There is excellent correspondence between observed and calculated values confirming the presence of the α phase.

Fig. 7(b) shows the map of the scattered X-ray intensity for fibres of the random terpolymer which have been hot

drawn at 40 °C to an extension ratio of 8 and then annealed at 80 °C. The equatorial section contains three peaks at $|Q| \sim 1.16, 1.52,$ and 2.00 \AA^{-1} and peaks at $|Q| \sim 1.20$ and 2.14 \AA^{-1} in the meridional section. The pattern has many features in common with that for the poly(L-lactide) although there is clearly a much larger non-crystalline component as can be seen from the diffuse isotropic scattering centred on $|Q| \sim 1.2 \text{ \AA}^{-1}$. Although the structure

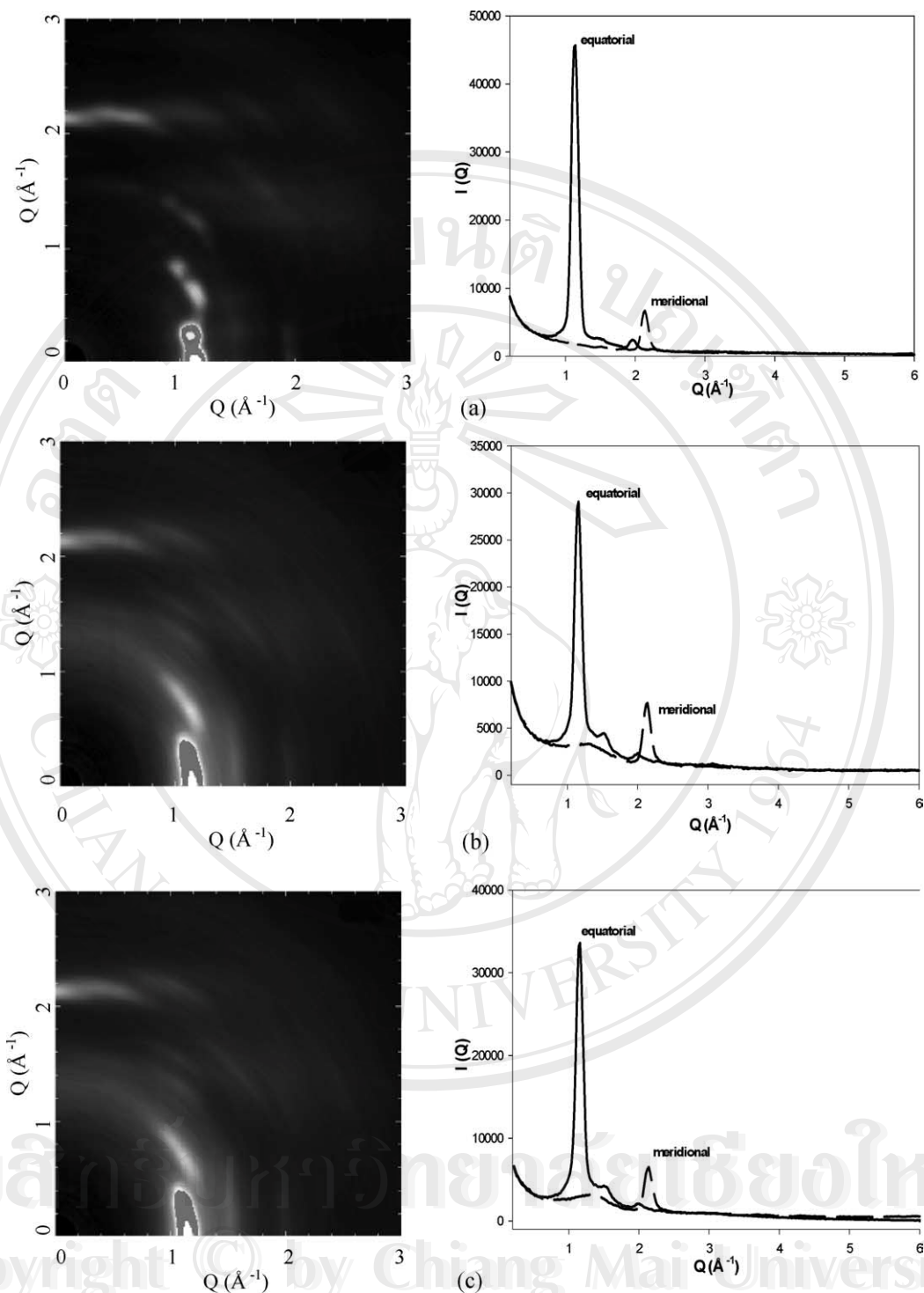


Fig. 7. X-ray scattering intensity maps $I(Q, \alpha)$ for the annealed fibres of (a) poly(L-lactide), (b) random terpolymer and (c) block terpolymer. In each case the fibre axis is vertical. The grey scale representation is arranged to that white represents the highest intensity. Note that the grey scale has been truncated to allow the details within the pattern to be observed. The relative strength of the strong equatorial feature at $|Q| \sim 1.2 \text{ \AA}^{-1}$ can be judged from the equatorial section. The accompanying line plots show the equatorial ($\alpha=0^\circ$, full line) and the meridional section ($\alpha=90^\circ$, broken line).

is somewhat smeared, probably as a result of somewhat smaller crystals, it is clear that the pattern of intensity of the sharper crystalline features observed for the poly(L-lactide) are reproduced in the random terpolymer pattern. The positions of the $hk0$ reflections, the layer

line spacing and the distribution of intensity along each layer line (Fig. 8(b)) are more or less equivalent between homopolymer and random terpolymer although the sparsity of higher order $hk0$ reflections makes calculation of the unit cell for the latter rather

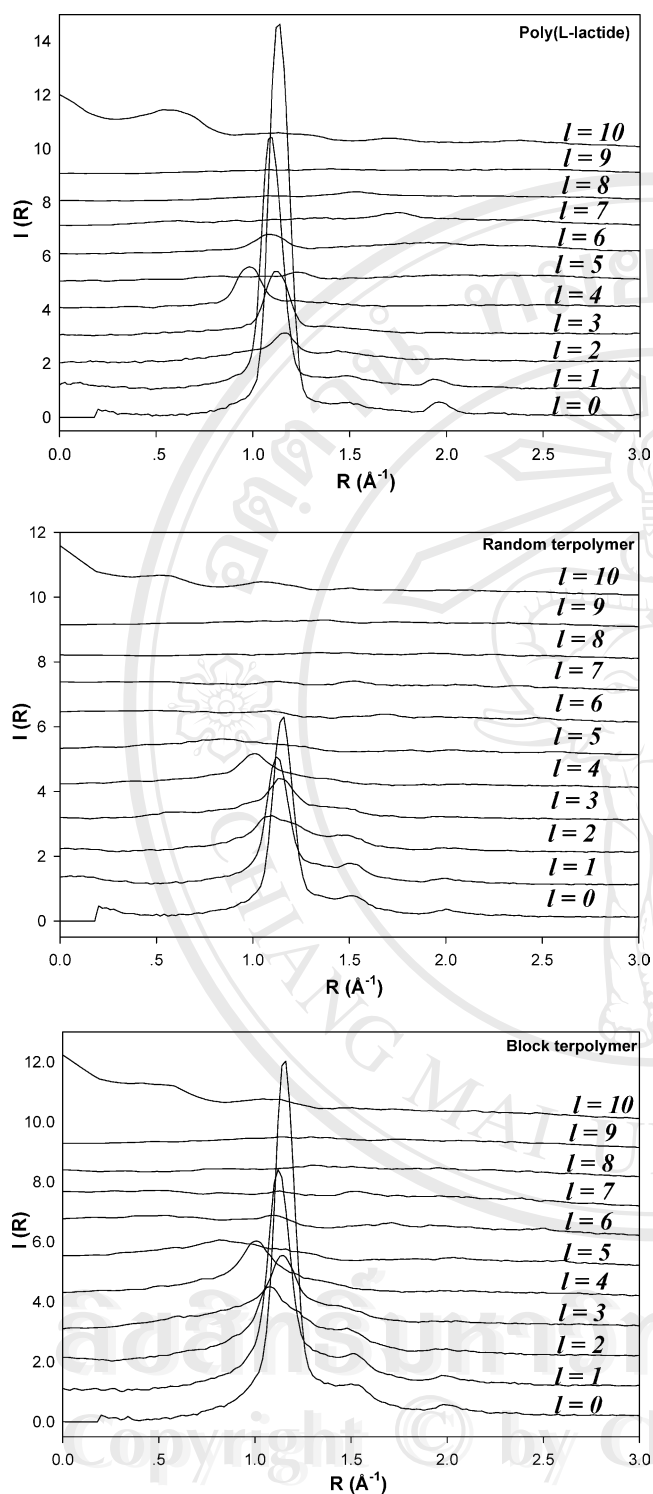


Fig. 8. Cross sections of the intensity maps shown in Fig. 7 taken at constant Z values corresponding to the layer line number indicated in the figures.

imprecise. However, it is clear that the crystal structure is equivalent to the α phase of poly(L-lactide).

A similar pattern of observations can be made with respect to the intensity map for the block copolymer (Fig. 7(c)). The block copolymer exhibits three peaks at $|Q| \sim 1.16, 1.52$ and 1.98 on the equatorial section and two

peaks ~ 1.30 and 2.14\AA^{-1} on the meridional axis. Again a comparison of the features including the layer line intensity distributions (Fig. 8) confirms the presence of a crystal structure equivalent to the α phase of poly(L-lactide). The strong equatorial feature at $|Q| \sim 1.2 \text{\AA}^{-1}$ which corresponds to the 110 peak in the α phase and is present in all three fibre patterns has a breadth at half height of $\sim 0.15 \text{\AA}^{-1}$. A similar breadth is observed for the 0, 0, 10 reflection on the meridian. This corresponds to crystal sizes of the order of 50\AA , although we have not corrected for any instrumental broadening.

For the α phase of poly(L-lactide), meridional reflections should be limited to the 10th, 20th etc layer lines. A number of authors have reported the presence of meridional reflections on other layer lines which they have interpreted as arising from non-integer helices and variation in the up-down symmetry of neighbouring chains [9–11,14]. For the poly(L-lactide) annealed fibre we observed some very weak scattering on the 7th layer line on the meridional axis. However, as with Sasaki et al. [14] we have attributed this to streaking from nearby reflections on the same layer line. Other than a very weak reflection at $\sim 4.30 \text{\AA}^{-1}$ corresponding to the 20th layer line, we did not observe meridional reflections on any other layer lines.

The small-angle X-ray scattering pattern for the as-spun filaments of the random or block terpolymer shows no distinctive features other than a small level of continuous scattering from simple density fluctuations. This suggests that the block copolymer does not exhibit any microphase segregation in the melt. This is not surprising as there will be quite a broad distribution of the block lengths from one polymer chain to another. In contrast, the patterns recorded for the annealed fibres show very strong and highly anisotropic scattering features as shown in Fig. 9. For the random copolymer (Fig. 9(a)) we see very sharp meridional peaks indicating a highly aligned two phase structure. The azimuthal variation of intensity is probably defined by the resolution of the instrument rather than any slight misorientation of the crystallites. The peak position is 0.038\AA^{-1} and the peak width is 0.01\AA^{-1} . There is also an equatorial streak which probably arises from micro voids in the original as-spun fibre which have been extended during hot drawing. The block copolymer fibre shows a similar pattern but the scattering is very much weaker with maxima at 0.031\AA^{-1} and a peak width of 0.02\AA^{-1} .

The WAXS and SAXS data provides a detailed view of the multiple phase morphology. For both terpolymers the crystallites are formed from the lactide units. There is no evidence for any crystal structure corresponding to that exhibited by poly(caprolactone) [35]. The lactide units crystallise in a structure equivalent to the α phase of poly(L-lactide). The block terpolymer crystallises more rapidly presumably due to the greater mobility of the end blocks but the random terpolymer displays a highly developed lamellar stack type SAXS pattern, suggesting better defined crystals than in the block copolymer system where the equivalent

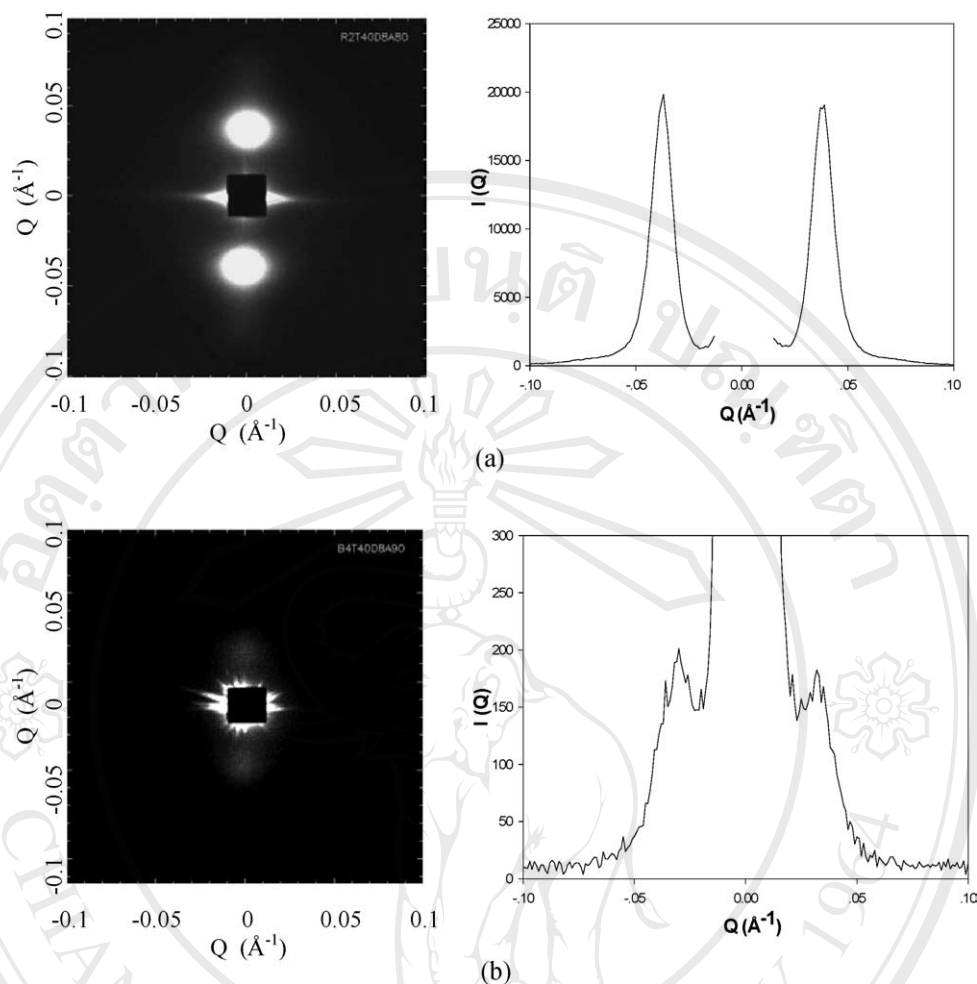


Fig. 9. Small-angle X-ray scattering patterns recorded for the same annealed fibres as in Fig. 7 i.e. (a) annealed random terpolymer and (b) annealed block copolymer. In each case the fibre axis is vertical. The dark square in the centre is the shadow of the beam stop. In Fig. 9(b), the scattering is much weaker than in Fig. 9(a) and some scattering from the collimation system can be seen around the beam stop in the form of short spikes.

SAXS is rather weak. The SAXS patterns give long periods of the order of 160 \AA for the random terpolymer and 200 \AA for the block terpolymer. With crystallinity levels as recorded in Fig. 6, this suggests crystal sizes of the order of 40 \AA similar to those derived from the meridional peaks. The lactide sequence in either the random or terpolymer determined by NMR is of the order of 10 which corresponds to 60 \AA for a chain in a 10/3 helix conformation.

7. Structure of un-annealed samples

Although the annealed fibre patterns are an excellent basis for structural analysis, such fibres are unsuitable for use as absorbable sutures as they are too stiff and exhibit a high level of crystallinity. In Fig. 10 we show the X-ray scattering patterns for the random and block terpolymers prepared under conditions (low draw ratio, low draw temperature, no annealing) which yield filaments more suited for use as absorbable sutures [2]. Comparison of these patterns with those for the annealed fibres (Fig. 7) reveals a

greater extent of azimuthal arcing indicating a lower level of orientation. This serves to smear the features. We can identify an intense feature on the equatorial sections at $Q = 1.16 \text{\AA}^{-1}$ and a rather weaker meridional feature at $Q = 2.14 \text{\AA}^{-1}$ in the pattern for the random terpolymer. The block terpolymer pattern exhibits an intense equatorial feature at $Q = 1.16 \text{\AA}^{-1}$ and a meridional feature at $Q = 2.18 \text{\AA}^{-1}$. The breadth of the equatorial peak for the block copolymer ($\Delta Q = 0.34 \text{\AA}^{-1}$) is about twice that observed for the equivalent peak in the pattern for the random terpolymer. The breadths of the meridional features are $\Delta Q = 0.31 \text{\AA}^{-1}$ for the block terpolymer and $\Delta Q = 0.25 \text{\AA}^{-1}$ for the random terpolymer.

Comparison of the fibre patterns with the equivalent patterns recorded for the annealed fibres suggests that the structures are similar but clearly we can not identify directly the well defined layer lines present in Fig. 8. Extracting structural information from fibre patterns with partial alignment is a long standing problem and a variety of techniques have been proposed. Most methods focus on procedures to deconvolute the observed pattern with the

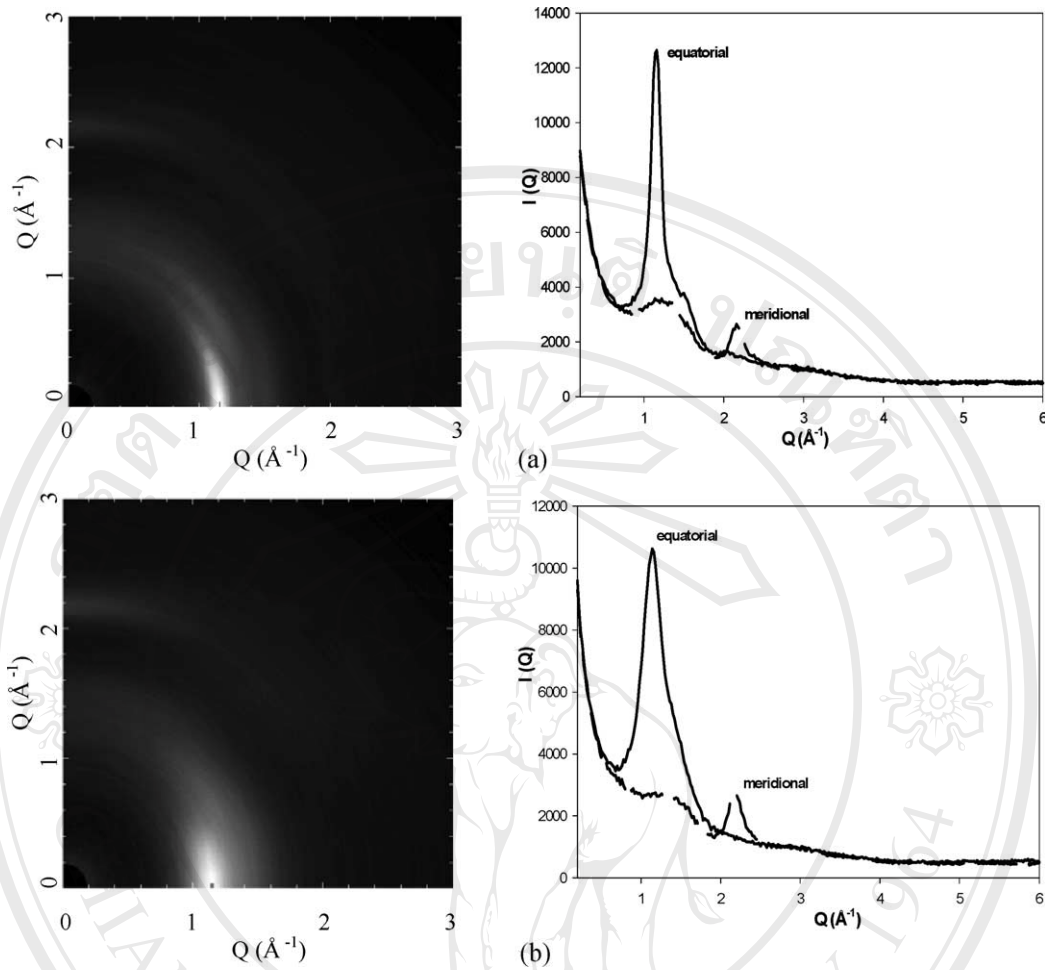


Fig. 10. X-ray scattering intensity maps $I(Q, \alpha)$ for the unannealed fibres of (a) random terpolymer and (b) block terpolymer. In each case the fibre axis is vertical. The grey scale representation is arranged to that white represents the highest intensity. Note that the grey scale has been truncated to allow the details within the pattern to be observed. The relative strength of the strong equatorial feature at $|Q| \sim 1.2 \text{ \AA}^{-1}$ can be judged from the equatorial section. The accompanying line plots show the equatorial ($\alpha=0^\circ$, full line) and the meridional section ($\alpha=90^\circ$, broken line).

estimated orientation distribution. Such approaches usually run in to problems concerned with estimating the orientation distribution function and in the numerical processing. We have used a somewhat simpler but rather novel approach which is introduced below.

The scattering for a fibre sample exhibiting a partial level of preferred orientation, $I(|Q|, \alpha)$, can be written as the convolution of the scattering for a perfectly aligned system $I^0(|Q|, \alpha)$ with the orientation distribution function $D(\alpha)$:

$$I(|Q|, \alpha) = I^0(|Q|, \alpha)D(\alpha) \quad (2)$$

The function $D(\alpha)$ describes the distribution of the structural units with respect to the symmetry axis of the sample.

If we express the intensity functions and the orientation distribution function in terms of a series of spherical harmonics, $I_{2n}(|Q|)$, $I_{2n}^0(|Q|)$ and D_{2n} we can write this convolution as [36,37]:

$$I_{2n}(|Q|) = \left\{ \frac{2\pi}{(4n+1)} \right\} D_{2n} I_{2n}^0(|Q|, \alpha) \quad (3)$$

where $n=0, 1, 2, 3 \dots \infty$. We only need the even terms of each series as the pattern will exhibit an inversion centre intrinsic to an X-ray scattering pattern for a non-absorbing fibre. The components of each series can be obtained by [37]:

$$I_{2n}(|Q|) = (4n+1) \int_0^{\pi/2} I(|Q|, \alpha) P_{2n}(\cos \alpha) \sin \alpha \, d\alpha \quad (4)$$

and related expressions, where $P_{2n}(\cos \alpha)$ are a series of spherical harmonics [37], for example, $P_0=1$, $P_2(\cos \alpha) = (3 \cos^2 \alpha - 1)/2$. The complete scattering pattern may be recovered by:

$$I(|Q|, \alpha) = \sum_{2n=0}^{2n=\infty} I_{2n}(|Q|) P_{2n}(\cos \alpha) \quad (5)$$

The value of this representation is that the effects of preferred orientation are separated from the dependence of

the scattering on the spatial correlations [37,38]. Eq. (3) shows that for samples with the same structure, the variation of the amplitudes of the spherical harmonics $I_{2n}(|Q|)$ with $|Q|$ are essentially the same, with a simple constant multiplier dependent on the level of preferred orientation. The orthogonal nature of the spherical harmonics in Eq. (3) means that for multiple phase structures as considered here, where the scattering from the different phases is additive, the resultant spherical harmonics will also be linear combinations of the harmonic functions for each phase.

To check the efficacy of this approach, we have compared the first four components (Fig. 11) of the series of spherical harmonics derived from the patterns shown in Fig. 7, i.e. the annealed fibres. The weight of any feature in a harmonic is a function of the fraction of the material which exhibits that structure and the level of preferred orientation as well as the relative strength of the underlying structure factor.

We identified above, that the structure in each fibre contains an anisotropic structure which involves both crystalline and non-crystalline components and some isotropic scattering from a unoriented amorphous structure.

The spherical harmonics for $2n > 0$ represent the anisotropic scattering and hence they will contain only the crystalline and aligned non-crystalline scattering. If we compare the three curves each of Fig. 11(a)–(d) it is clear that each of the features (i.e. maxima and minima) observed in the appropriate spherical harmonic are reproduced in the equivalent functions derived from the scattering for the two terpolymers. The variations in height reflect the small differences in preferred orientation between the three fibre samples. The curves for $2n=0$ (Fig. 11(a)) show larger differences due to the variations in crystallinity between the three samples as reflected most clearly in the height of the sharp peak at $|Q| = 1.18 \text{ \AA}^{-1}$. Despite such differences in weightings, we can discern that the various features present in the poly(L-lactide) sample are also present in the equivalent curves for the two terpolymer fibres. These observations underpin the observations already made above using the complete patterns and the layer line plots. Clearly the method is effective and does not require any assumption about the orientation distribution function or numerical approximations.

Fig. 12 shows the first four spherical harmonic

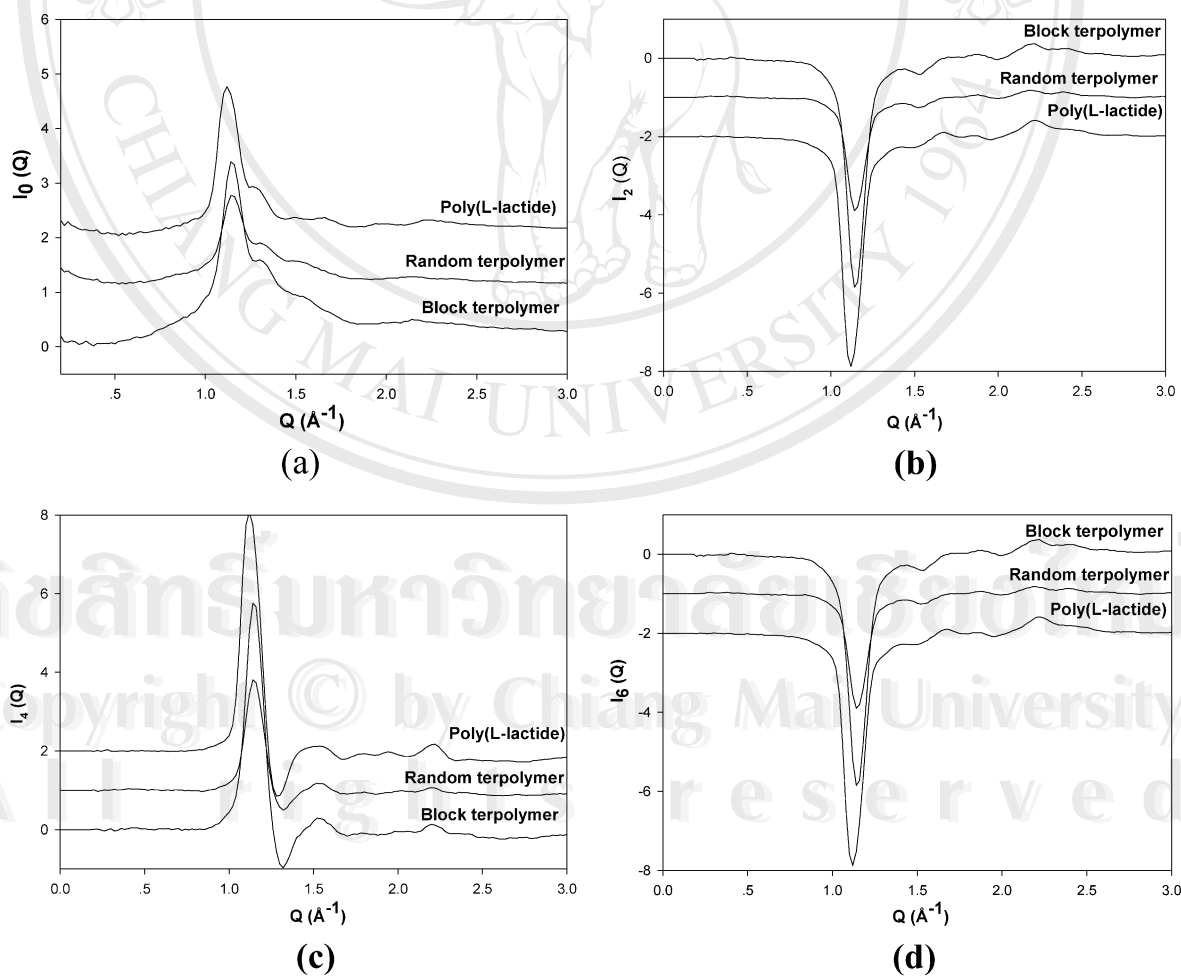


Fig. 11. A comparison of the amplitudes of the series of spherical harmonics which represent the fibre patterns shown in Fig. 7 for the annealed samples of the poly(L-lactide), the random and block terpolymers. Each curve has been offset for clarity but in all cases the value of the functions at $|Q| = 0.0 \text{ \AA}^{-1}$ is zero.

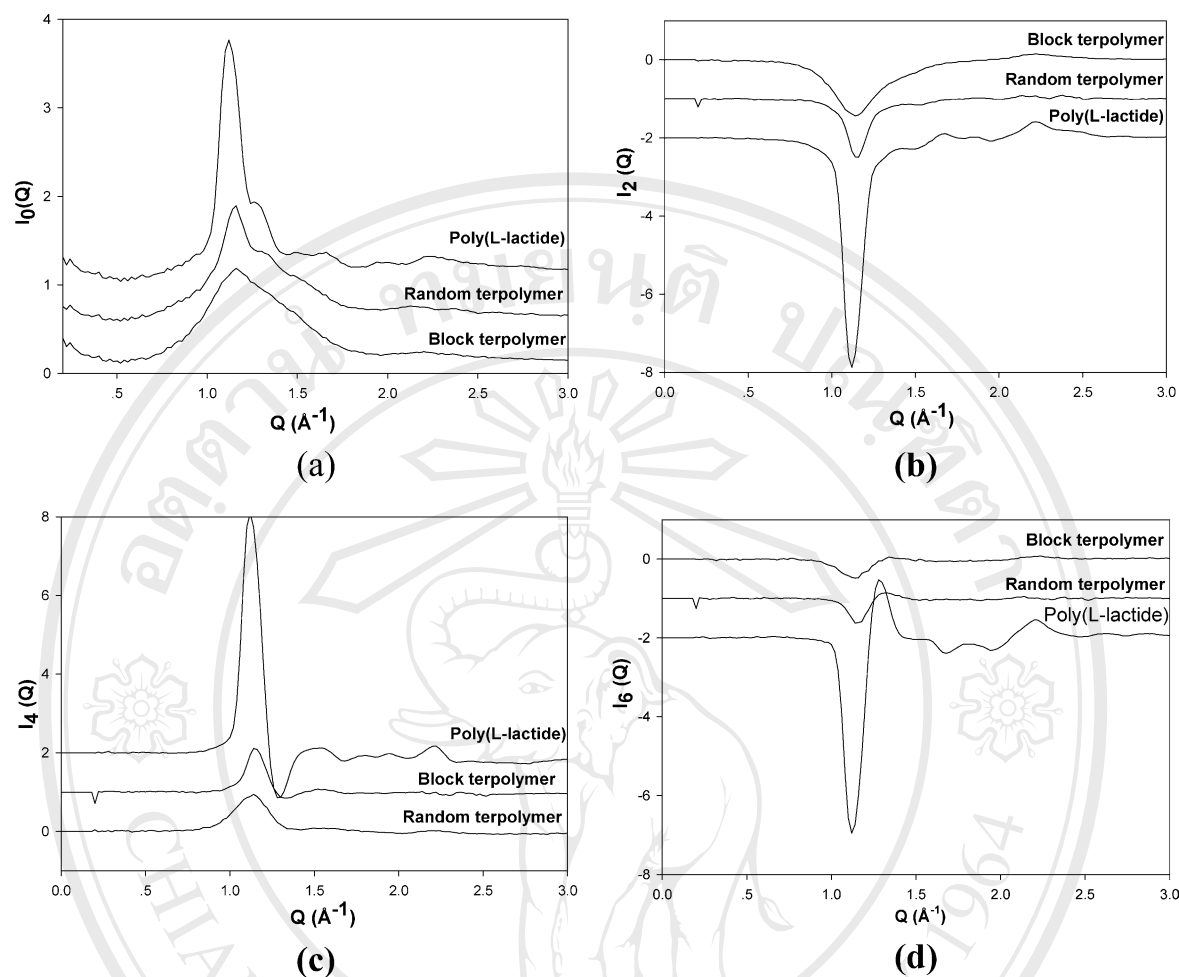


Fig. 12. A comparison of the amplitudes of the series of spherical harmonics which represent the fibre patterns shown in Fig. 10 for the unannealed samples of the random and block terpolymers with those derived from the annealed poly(L-lactide) shown in Fig. 7.

components derived from the scattering patterns shown in Fig. 10 compared to those derived from the scattering pattern of the poly(L-lactide) shown in Fig. 7(a). If we consider the curves for $2n > 0$ it is clear that the features for the poly(L-lactide) are very much more intense than those observed in the curves relevant to the terpolymer fibres. This simply reflects the higher proportion of anisotropic material and the higher level of preferred orientation present in the poly(L-lactide) fibre. In terms of the key minima and maxima ($|Q| = 1.18, 1.3$ and 2.4\AA^{-1}), the curves are equivalent indicating that it is reasonable to conclude that the terpolymer filaments prepared at low draw ratios and without annealing exhibit a similar crystal structure to poly(L-lactide) despite the smaller crystal size and greater crystal misorientation.

8. Structure of un-drawn fibres

In order to confirm that the drawing does not induce any changes to the crystal structure other than the level of preferred orientation and degree of crystallinity, we have

crystallised samples of the three polymers from quiescent melts and recorded the X-ray scattering intensity as a function of $|Q|$ using the same diffractometer as employed to record the fibre scattering data. The fully corrected and scaled intensity functions are shown in Fig. 13.

In order to compare the scattering from these isotropic samples with that from the fibres we have calculated the scattering expected for an isotropic sample with the same structure as the hot-drawn fibres. Experimentally, this would be achieved by powdering the fibre in to small parts which are then arranged randomly. It is more straightforward to perform the azimuthal averaging numerically using the scattering pattern for each fibre. The scattering pattern for a sample containing the same fibrous structure but with the fibre axis arranged at every angle possible with respect to the scattering vector is given by:

$$I_{\text{isotropic}}(Q) = \int_0^{\pi/2} I(Q, \alpha) \sin \alpha d\alpha \quad (7)$$

Comparison of Eqs. (4) and (7) shows that $I_{\text{isotropic}}(Q)$ is equivalent to $I_0(Q)$ (as in Figs. 11 and 12) and these functions are also plotted in Fig. 13. We can see that the

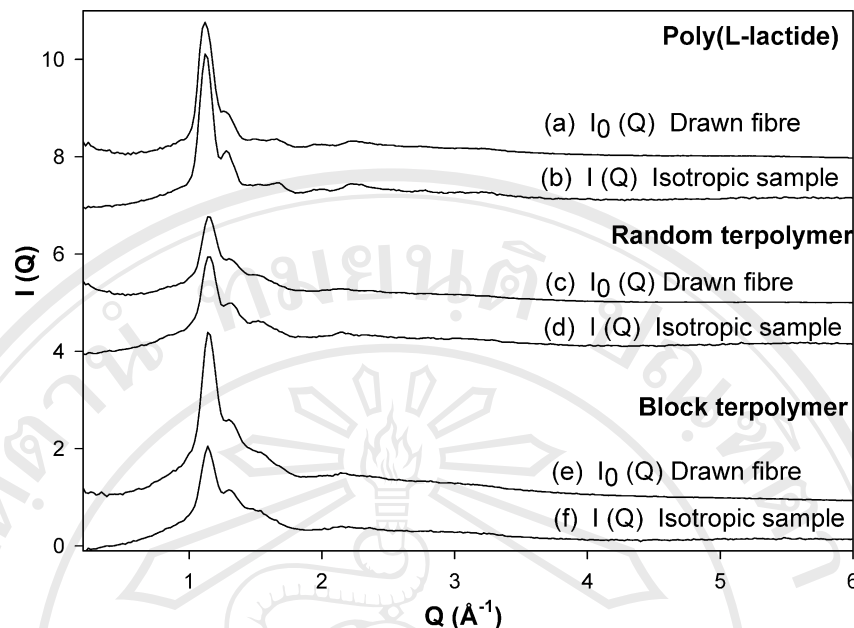


Fig. 13. Plots of the fully corrected and scaled wide-angle X-ray scattering intensity $I(Q)$ recorded for samples of poly(L-lactide) (PLLA), random terpolymer and block terpolymer crystallised from a quiescent melt compared to the azimuthally averaged data $I_0(Q)$ for each annealed fibre as described in the text. The azimuthally averaged data represents a sample with no global preferred orientation but the same localised structure as the fibres.

curves are essentially the same in terms of peak positions and overall shapes. In the case of the block terpolymer, the height of the intense peak at $|Q| \sim 1.2 \text{ \AA}^{-1}$ in the curve for the isotropic sample is somewhat smaller than derived from the fibre pattern showing that that hot-drawing and annealing has increased the level of crystallinity. This effect is very much less marked in the case of the random terpolymer and in poly(L-lactide).

9. Discussion

Fibre diffraction studies are conventionally performed on highly aligned fibres which have often been extensively treated to enhance the levels of crystallinity; the work of Sasaki et al. [14] is an example where the fibre has been treated to degrade the polymeric structure in order to enhance the crystallinity. In this work we have introduced a new tool in the study of fibres which allows the X-ray scattering patterns for structures with differing levels of preferred orientation to be compared directly without recourse to arbitrary processes or the separation into the scattering from phases. The method employs a representation of the data as a series of spherical harmonics. The methodology has been applied to two terpolymers with rather different architectures but both involving sequences of randomly distributed lactide units with sequence lengths of ~ 10 , although their positioning in the molecular chain differs. We have prepared highly drawn monofilaments which have shown that both systems exhibit a semi-crystalline structure in which the lactide units crystallise

in a structure equivalent to the α phase of poly(L-lactide). Of course there are some limitations to this novel approach but the two annealed terpolymer fibres exhibit structures equivalent to the α phase of poly(L-lactide). The helical structure of the lactide sequences does not appear to be distorted as no systematically absent 00l type reflections were observed. This contrasts with studies of the poly(L-lactide) homopolymer [14] and may arise from the less specific chain interactions which may be present in the rather more disordered copolymer structures. These weaker interchain interactions make a specific regular chain conformation more likely.

A particular feature of this new approach, is that we can study the crystalline structure of fibres more relevant to application, for example with the biodegradable terpolymers studied here, use as absorbable sutures is promising application. In the low draw ratio terpolymer fibres, it is clear that despite the lower level of orientation and rather small crystal size ($\sim 20\text{--}30 \text{ \AA}$) the crystal structure remains largely the same. Comparison of the annealed and unannealed fibre patterns and associated sections shows the significant effect of annealing on the apparent crystal size. This is more marked for the block copolymer system. Comparison of scattering obtained from samples prepared via a quiescent melt phase shows that the drawing process does not affect the crystal structure but it does influence the level of crystallinity most markedly in the block copolymer system. This system exhibits a maximum in the crystallisation rate for quiescent systems at a slightly higher temperature than that recorded for the random terpolymer. This can be related to the differences in T_m and T_g for the

two terpolymers, essentially the peak crystallisation rates occur at the same level of undercooling midway between T_m and T_g . We attribute the increased level of crystallinity in the case of the block terpolymer after drawing to the enhanced mobility of the end blocks in the block copolymer system. We did not see any evidence that there was micro phase segregation in the block terpolymer melt prior to hot drawing which might also influence the rate of crystallisation. However, it is clear that on the larger scale the two phase crystalline/non-crystalline structure is rather ill-defined in the block copolymer case. We attribute this to the range of block lengths present in the polymer chains and the rather disrupting (i.e. non-inclusion) effect of the highly disordered central block containing very short sequences of both lactide and caprolactone. In contrast, the random copolymer exhibits a rather well defined two-phase structure which we attribute to the greater extent that non-lactide units can be incorporated in to the interfaces of lamellar crystals to provide a smoother crystal face. This variation in the structure and dynamics of two materials with similar chemical composition but rather different architectures will be most helpful in the optimisation of these materials for use in biomedical applications.

10. Summary

Random or block terpolymers containing ~70 mol% of lactide units with a balance of caprolactone and glycolide moieties exhibit a semi-crystalline structure in which the crystal component is essentially equivalent to the α crystal phase of poly(L-lactide). The crystal structure appears to be largely invariant to different processing conditions for as to whether the terpolymer is crystallised under quiescent conditions or hot-drawn from pre-spun filaments to low or high draw ratio. This contrasts with the behaviour of the poly(L-lactide) homopolymer which exhibits a number of crystal forms, although the fibres prepared in this work under similar conditions to those used for the terpolymers also generates the α form. The level of crystallinity is enhanced in the block terpolymer samples which are subjected to hot drawing but this is not the case for the random copolymer. In contrast, the random copolymer appears to have a very much better defined lamellar structure which we attribute to the ability of the random copolymer to incorporate minor levels of the other units in to the crystal interface in order to achieve a smoother crystal surface. The use of the spherical harmonic representation of the fibre patterns considerable facilitates comparison between the annealed and unannealed fibres and samples crystallised from quiescent melts. This is particularly important for understanding the chemistry-structure-property relationships in these complex disordered polymer monofilaments with potential for use as absorbable sutures.

Acknowledgements

This work was supported by the National Metal and Materials Technology Centre (MTEC), Thailand and the Royal Society, UK, through the award of South-East Asia Fellowship to JS. The small-angle X-ray scattering data were obtained using beam-line 16.1 at the CCLRC Daresbury synchrotron radiation source and we thank the beam-line scientist Anthony Gleeson for his help with the SR experiments. We thank the Thai Ministry of University Affairs and the Graduate School, Chiang Mai University for financial support.

References

- [1] Bezwada RS, Jamiolkowski DD, Lee IY, Agarwal V, Persivale J, Trenkenthin S, et al. *Biomaterials* 1995;16:1141–8.
- [2] Buntner B, Nowak M, Kasperczyk J, Ryba M, Grieb P, Walski M, et al. *J Control Release* 1998;56:159–67.
- [3] Cai Q, Bei JZ, Wang SG. *Polym Adv Technol* 2002;13:105–11.
- [4] Cai Q, Bei JZ, Wang SG. *Polymer (B)* 2002;43:3585–91.
- [5] Dawes E, Rushton N. *Biomaterials* 1997;18(24):1615–23.
- [6] Cordewener FW, Dijkgraaf LC, Ong JL, Agrawal CM, Zardeneta G, Milam SB, et al. *J Biomed Mater Res* 2000;50:59–66.
- [7] Hasirci V, Lewandrowski KU, Bondre SP, Gresser JD, Trantolo DJ, Wise DL. *Bio-Med Mater Eng* 2000;10:19–29.
- [8] Honda M, Yada T, et al. *J Oral Maxillofacial Surgery* 2000;58(7):767–75.
- [9] De Santis P, Kovacs J. *Biopolymers* 1968;6:299–306.
- [10] Hoogsteen W, Postema AR, Pennings AJ, ten Brinke G, Zugenmaier P. *Macromolecules* 1990;23:634–42.
- [11] Kobayashi J, Asahi T, Ichiki M, Oikawa A, Suzuki H, Watanabe T, et al. *J Appl Phys* 1995;77:2957–73.
- [12] Cartier L, Okihara T, Ikada Y, Tsuji H, Puiggali J, Lotz B. *Polymer* 2000;21:8909–19.
- [13] Puiggali J, Ikada Y, Tsuji H, Cartier L, Okihara T, Lotz B. *Polymer* 2000;21:8921–30.
- [14] Sasaki A, Asakura T. *Macromolecules* 2003;36:8385–90.
- [15] Cai Q, Bei JZ, Wang SG. *Acta Polym Sin* 1999;761–4.
- [16] Srisa-ard M, Molloy R, Molloy N, Siripitayanon J, Sriyai M. *Polym Int* 2001;50:891–6.
- [17] Cai Q, Bei JZ, Wang SG. *Polym Adv Technol* 2000;11:159–66.
- [18] Nijenhuis AJ, Grijpma DW, Pennings AJ. *Macromolecules* 1992;25:6419–24.
- [19] Flory PJ. *J Chem Phys* 1947;15:684.
- [20] Flory PJ. *J Chem Phys* 1949;17:223.
- [21] Windle AH, Viney C, Golombok R, Donald AM, Mitchell GR. *Faraday Discuss* 1985;79:55.
- [22] Dobrzynski P. *J Polym Sci, Part A: Polym Chem* 2002;40:3129–43.
- [23] Kasperczyk J, Bero M. *Makromol Chem* 1991;192:1777–87.
- [24] Bero MJ, Kasperczyk J, Adamus G. *Makromol Chem* 1993;194:907–12.
- [25] Kasperczyk J, Bero M. *Makromol Chem* 1991;194:913–25.
- [26] Kasperczyk J, Bero M. *Makromol Chem* 1993;194:913–25.
- [27] Mitchell GR. In: Allen G, Bevington J, editors. *Comprehensive polymer science*, vol. 1. New York: Pergamon Press; 1989. p. 687–729 [chapter 31].
- [28] Bassett D. *J Macromol Sci Phy* 2003;B42:227.
- [29] Sarasua JR, Prud'homme RE, Wisniewski M, Le Borgne A, Spassky N. *Macromolecules* 1998;31:3895–905.
- [30] Vasanthakumari R, Penning JA. *Polymer* 1983;24:175–8.
- [31] Tsuji H, Ikada Y. *Polymer* 1995;36:2709–16.

- [32] Walsh DR. In: Booth C, Price C, editors. Comprehensive polymer science, vol. 2. New York: Pergamon Press; 1989. p. 135 [chapter 5].
- [33] Perrin DE, English J. In: Domb AJ, Kost J, Wiseman DM, editors. Handbook of biodegradable polymers. New York: Harwood Academic Publishers; 1997. p. 3 [chapters 1 and 3].
- [34] Fischer EW, Serzel HJ, Wegner G. Kolloid Z Polym 1973;251:980.
- [35] Chatani Y, Okita Y, Tadokoro H, Yamashita Y. Polym J 1970;1: 555–62.
- [36] Lovell R, Mitchell GR. Acta Cryst 1981;A37:135.
- [37] Mitchell GR, Windle AH. Colloid Polym Sci 1982;260:754.
- [38] Mitchell GR, Saengsuwan S, Bualek-Limcharoen S. Prog Colloid Polym Sci 2005;130.



ลิขสิทธิ์มหาวิทยาลัยเชียงใหม่
Copyright © by Chiang Mai University
All rights reserved

JOURNAL PUBLICATIONS

entitled

**Investigation of the Crystal Structure in
Segmented Triblock L-lactide,
 ϵ -caprolactone and Glycolide
Terpolymer Fibers**

published in the journal

ลิขสิทธิ์มหาวิทยาลัยเชียงใหม่

Copyright © Chiang Mai University

All rights reserved

(www.science.cmu.ac.th/journal-science/josci.html)

(Chiang Mai J. Sci. 2005; 32(3) : 507-513)

มหาวิทยาลัยเชียงใหม่
CHANG MAI UNIVERSITY

Investigation of the Crystal Structure in Segmented Triblock L-Lactide, ϵ -Caprolactone and Glycolide Terpolymer Fibres

Wasinee Channuan [a], Jintana Siripitayananon* [a], Robert Molloy [a], Montira Sriyai [a] and Geoffrey R. Mitchell [b]

[a] Biomedical Polymers Technology Unit, Department of Chemistry, Faculty of Science, Chiang Mai University, Thailand 50200

[b] Polymer Science Centre, Department of Physics, University of Reading, Whiteknights, Reading RG6 6AF, UK

* Author for correspondence, e-mail : jin-sc@chiangmai.ac.th

Reprinted

Chiang Mai
Journal of
Science



ลิขสิทธิ์มหาวิทยาลัยเชียงใหม่

Copyright © by Chiang Mai University

Journal of the Science Faculty of Chiang Mai University

ISSN 0125-2526

<http://www.science.cmu.ac.th/journal-science/josci.html>



Chiang Mai J. Sci. 2005; 32(3) : 507-513
www.science.cmu.ac.th/journal-science/josci.html
Contributed Paper

Investigation of the Crystal Structure in Segmented Triblock L-Lactide, ϵ -Caprolactone and Glycolide Terpolymer Fibres

Wasinee Channuan [a], Jintana Siripitayananon* [a], Robert Molloy [a], Montira Sriyai [a] and Geoffrey R. Mitchell [b]

[a] Biomedical Polymers Technology Unit, Department of Chemistry, Faculty of Science, Chiang Mai University, Thailand 50200

[b] Polymer Science Centre, Department of Physics, University of Reading, Whiteknights, Reading RG6 6AF, UK

* Author for correspondence, e-mail : jin-sc@chiangmai.ac.th

ABSTRACT

Segmented triblock terpolymers of L-lactide, ϵ -caprolactone and glycolide have the ability to biodegrade by simple hydrolysis in the human body. They therefore have the potential for use in biomedical applications such as absorbable surgical sutures. The particular terpolymer studied in this research work had an overall composition of L-lactide : ϵ -caprolactone : glycolide = 70 : 25 : 5 mol %. Monofilament fibres of the terpolymer were produced by melt spinning using a small-scale fibre extrusion apparatus. Under the processing conditions used, which involved rapid cooling, the as-spun fibres were obtained in an almost completely "quenched amorphous" state. Subsequent off-line hot-drawing and annealing steps were then employed in order to induce crystallization and to build into the fibre the required degree of molecular orientation necessary to develop its mechanical properties. The dependence of these mechanical (tensile) properties on the processing conditions used was also studied, while X-ray diffraction (XRD) was used to determine molecular orientation and crystal structure. It was found that the crystal structure in the fibre after hot-drawing and annealing was predominantly that of the α -form of poly(L-lactide) and that it was this part of the matrix which was responsible for the fibre's tensile strength.

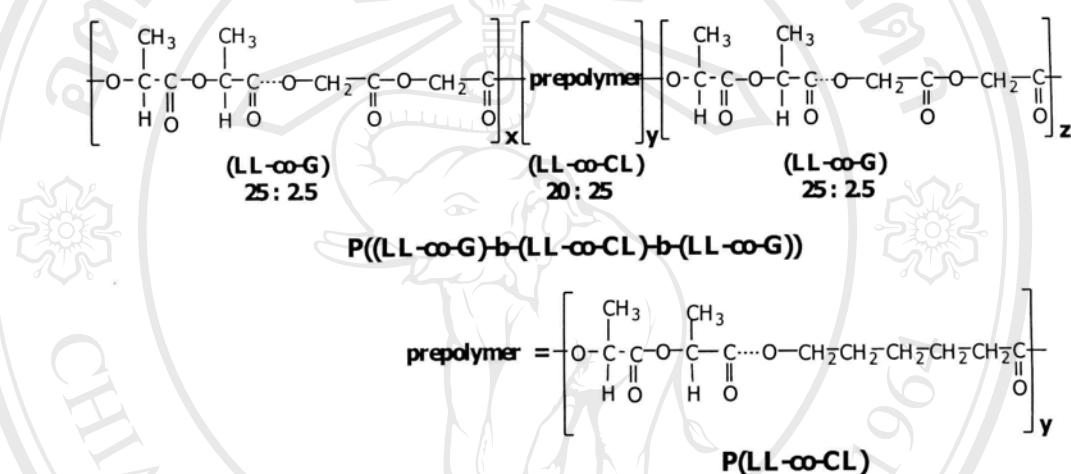
Keywords : absorbable monofilament surgical suture, biodegradable polyester, segmented triblock terpolyester.

1. INTRODUCTION

Absorbable surgical sutures can be classified into two groups : multifilaments and monofilaments. In this research, attention is focused on monofilaments. Monofilament sutures have less affinity for bacteria and a smooth surface which are major advantages in exhibiting less tissue reaction and tissue drag. However, they tend to be quite stiff and difficult to handle which are disadvantages. The objective of this work is to develop a new, relatively low-cost synthetic absorbable suture

with the appropriate balance of physical and mechanical properties. The polyester of particular interest in this work is a segmented triblock terpolymer of L-lactide (LL), ϵ -caprolactone (CL) and glycolide (G) with an overall composition of LL : CL : G = 70 : 25 : 5 mol %. L-Lactide is the major component due to its low cost while ϵ -caprolactone and glycolide increase chain flexibility and the degradation rate of the terpolymer respectively [1, 2]. The segmented triblock terpolymer consists of a soft centre block of a random

copolymer of LL and CL with a composition of LL : CL = 20 : 25 mol % and two hard end blocks of a random copolymer of LL and G with a combined composition of LL : G = 50 : 5 mol %. The molecular structure of the terpolymer is as shown below.



The soft centre-block provides good handling characteristics while the hard end blocks provide high strength. The strength provided by the end blocks comes from their ability to crystallize. One of our aims is to investigate the crystal structure in the fibre. Terpolymer fibres were produced by melt spinning followed by hot-drawing and annealing under appropriate conditions. The fibres obtained were then tested to evaluate their mechanical properties and X-ray diffraction techniques employed to determine their molecular orientation and crystal structure.

2. EXPERIMENTAL METHODS AND RESULTS

2.1 Materials

The segmented triblock terpolymer of L-lactide (LL), ϵ -caprolactone (CL) and glycolide (G) with a composition ratio 70 : 25 : 5 mol % was synthesized via a 2-step reaction employing procedures reported elsewhere [3-5]. The terpolymer was characterized by various analytical techniques : IR, $^1\text{H-NMR}$, $^{13}\text{C-NMR}$, GPC, DSC and TG. The results showed that $\overline{M}_w = 47,000$, $\overline{M}_w/\overline{M}_n =$

1.71, while the terpolymer composition of LL : CL : G = 71 : 24 : 5 mol %. From thermal analysis, $T_g = 41.7^\circ\text{C}$, $T_m = 156.3^\circ\text{C}$ (peak), $\Delta H_m = 25.2 \text{ J/g}$ and $T_d = 254 - 430^\circ\text{C}$ (weight loss range).

2.2 Fibre Processing

Monofilament fibres of the terpolymer were prepared by melt spinning using a small-scale melt spinning apparatus operating at 167°C and at an extrusion rate of 0.10 m/min. The fibre was extruded through a single hole, 1.0 mm diameter spinnerette, guided through an ice-water-cooling bath at $5-10^\circ\text{C}$, and then wound up on a spool at a take-up speed of 1.0 m/min. The fibre obtained, referred to as the "as-spun fibre", had an average diameter of $0.35 \pm 0.02 \text{ mm}$ and was characterized by DSC at a heating rate of $10^\circ\text{C}/\text{min}$. The results obtained are shown in Table 1. The as-spun fibre was then drawn to a draw ratio (λ) of 5.9 at 60°C at a draw rate of 2500 %/min. The hot-drawn fibre sample was also characterized by DSC at the same heating rate of $10^\circ\text{C}/\text{min}$. The results are also shown in Table 1.

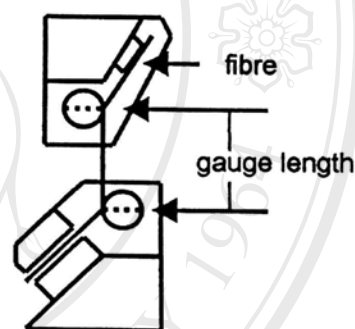
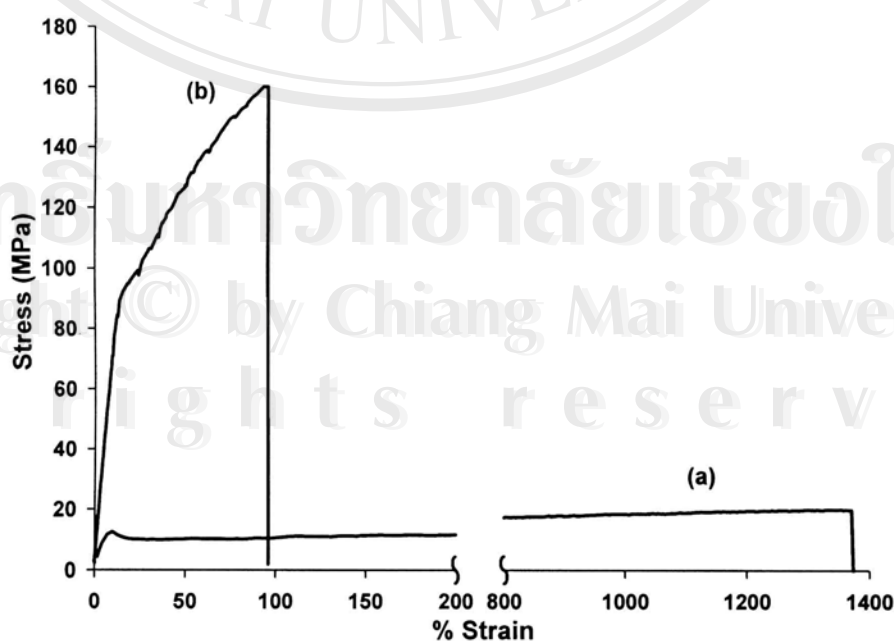
Table 1. Comparison of the thermal and mechanical properties of the as-spun and hot-drawn fibres.

Fibre sample	Thermal properties					Mechanical properties		
	T _c (°C)	T _m (°C)	ΔH _c (J/g)	ΔH _m (J/g)	ΔH _m -ΔH _c (J/g)	Stress at break (MPa)	Young's modulus (MPa)	Strain at break (%)
As-spun fibre	82.7	154.3	15.2	23.6	8.4	19	180	1417
Hot drawn fibre*	-	155.8	-	23.8	23.8	153	749	99

* The fibre was drawn to $\lambda = 5.9$ at 60°C with a draw rate of 2500 %/min

2.3 Mechanical Testing

The mechanical properties of both the as-spun and drawn fibres were measured at ambient temperature (22–25°C) using a Lloyds LRX+ Universal Testing Machine with an initial gauge length of 40 mm and a crosshead speed (initial strain rate) of 50 %/min. All tests were carried out with the fibre sample wound once around two bollard grips, as illustrated in Figure 1. The stress-strain curves obtained are shown in Figure 2 and the derived parameters, calculated as the averages of 4 readings, compared in Table 1.

**Figure 1.** Schematic diagram of the bollard grips showing the fibre sample mounted for tensile testing.**Figure 2.** Stress-strain curves for the (a) as-spun fibre and (b) the fibre drawn to $\lambda = 5.9$ at 60°C with a draw rate of 2500 %/min.

2.4 In-Situ Wide-Angle X-Ray Diffraction Experiments

To follow the changes in the fibre morphology during processing, a Synchrotron wide-angle X-ray diffraction (WAXD) technique was employed. Synchrotron measurements were carried out at Beamline Station 16.1 in the Rutherford Appleton Laboratory, UK. The wavelength of the X-ray beam used was 1.4 Å. The as-spun fibre sample was stretched in a temperature-controlled chamber of a tensiometer which permitted the focused X-rays to illuminate the same sample position during drawing. The

WAXD images were collected every 5 sec while the sample was being drawn at 60°C at a draw rate of 2500 %/min to a draw ratio (λ) of 9.8. The stress-strain curve and some selected WAXD patterns collected during drawing are shown in Figures 3(a)-(c). The effect of annealing was also studied by leaving the fibre at 60°C after being drawn. Figure 3(d) shows a WAXD pattern collected after annealing at 60°C for 10 min. For comparison, the same procedure was carried out with the fibre left to cool to room temperature. The corresponding WAXD pattern is shown in Figure 3(e).

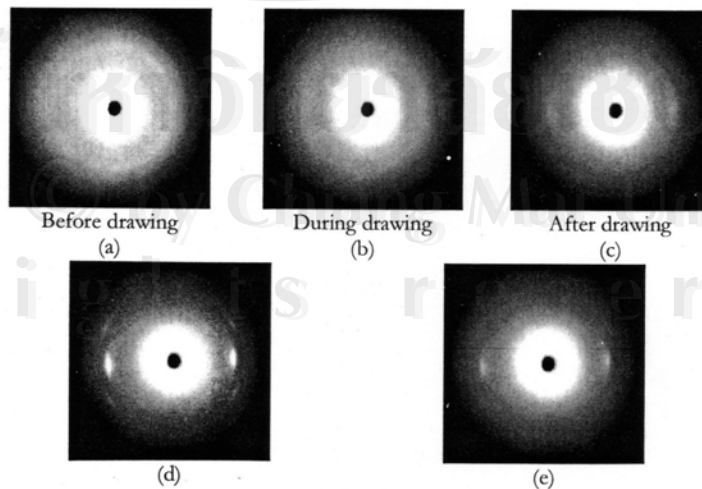
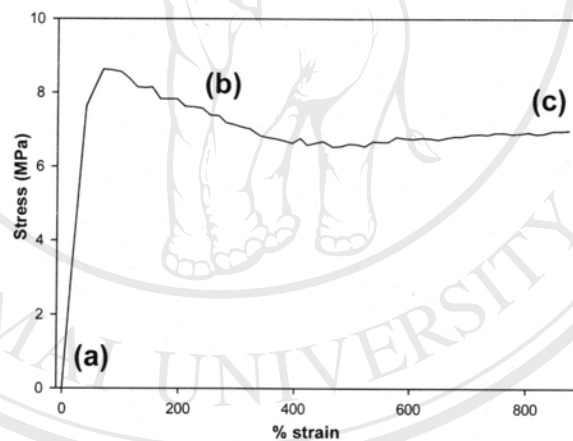


Figure 3. (a)-(c) : WAXD patterns collected during drawing at 60°C with a draw rate of 2500 %/min at the positions corresponding to those shown on the stress-strain curve shown above. (d) and (e) : The patterns collected after annealing at 60°C for 10 min and after leaving to cool at room temperature for 10 min respectively.

2.5 Crystal Structure Investigation

The crystal structure in the hot-drawn fibre was investigated by wide-angle X-ray scattering measurements. A symmetrical transmission diffractometer equipped with a graphite monochromator, pinhole collimation and a Cu K α source developed at the J.J. Thomson Laboratory, University of Reading, UK, was used.

Fibre samples were cut into 2 cm lengths and closely aligned in parallel to cover a 5 mm hole in an aluminum plate. The plate was then mounted so that the fibres were vertical and perpendicular to the X-ray beam. The scattering intensities for the drawn fibre were obtained as a function of scattering vector, $|Q|$, over the range 0.2 to 6 \AA^{-1} in steps of 0.02 \AA^{-1} and as a function of azimuthal angle, α , over the range 0 $^\circ$ to 90 $^\circ$ in steps of 2 $^\circ$ at

each position. $|Q|$ is defined as $4\pi\sin\theta/\lambda$, where 2θ is the angle between the incident and scattered beam and λ is the incident X-ray wavelength (1.54178 nm). The angle α is the angle between the fibre axis and the scattering vector. Figure 4(a) shows a 2D-scattering pattern of the segmented triblock terpolymer fibre which was drawn at 40 $^\circ\text{C}$ with a draw rate of 700 %/min to $\lambda = 8$ and annealed at 90 $^\circ\text{C}$ for 24 hrs. For comparison, Figure 4(b) shows a 2D-scattering pattern of a poly(L-lactide) homopolymer fibre which was drawn at 70 $^\circ\text{C}$ with a draw rate of 2400 %/min to $\lambda = 5$ and annealed at 90 $^\circ\text{C}$ for 24 hrs. The intensity profiles at different reciprocal lattice layers ($\lambda = 0-10$), as measured from the X-ray scattering patterns in Figure 4(a) and (b), are also shown in Figs. 4(c) and (d) respectively.

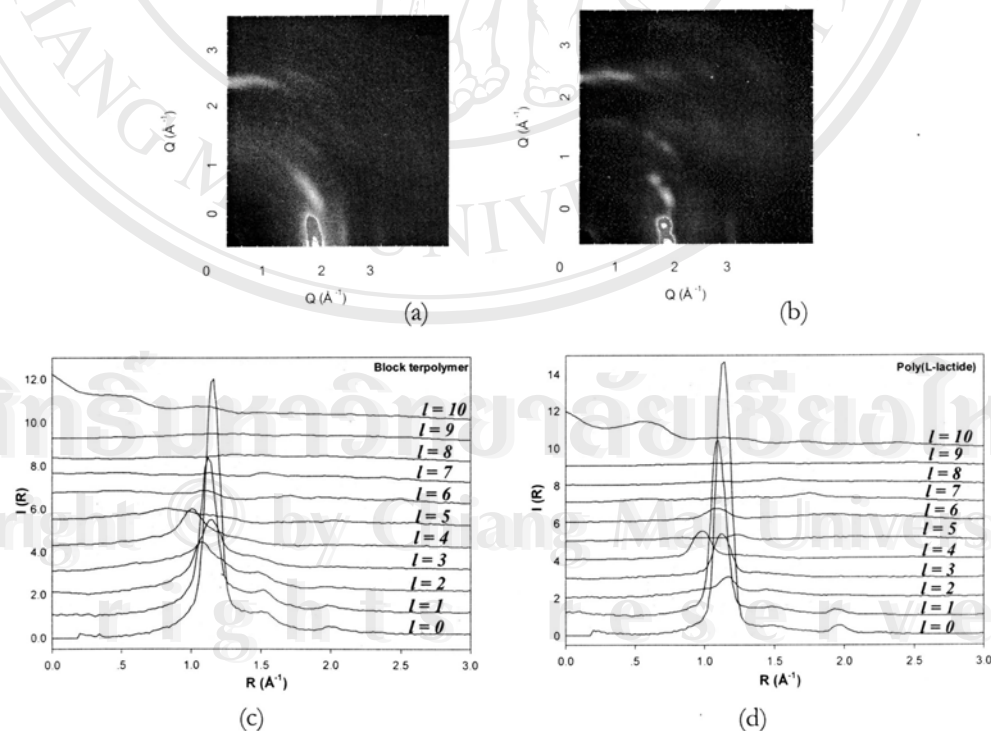


Figure 4. (a) XRD pattern for the terpolymer fibre drawn at 40 $^\circ\text{C}$ to $\lambda = 8$, followed by annealing at 90 $^\circ\text{C}$ for 24 hrs. (b) XRD pattern for a poly(L-lactide) fibre drawn at 70 $^\circ\text{C}$ to $\lambda = 5$, followed by annealing at 90 $^\circ\text{C}$ for 24 hrs. (c)-(d) Intensity profiles at different reciprocal lattice layers ($\lambda = 0 - 10$) corresponding to (a) and (b) respectively.

3. DISCUSSION

From mechanical testing, it was found that the fibre strength was significantly increased by hot-drawing, as seen in Figure 2 and Table 1. The strength of the fibre depends largely on its degree of crystallinity and molecular orientation [6-8]. Hot-drawing can induce both crystallization and molecular orientation. The degree of crystallinity of a fibre is directly proportional to its heat of melting, ΔH_m , which can be obtained from DSC. However, if the material crystallizes during the DSC heating scan, then the initial crystallinity of the fibre at the start of the scan is proportional to $\Delta H_m - \Delta H_c$ where ΔH_c is the heat of crystallization. Therefore, from Table 1, we can conclude that the drawn fibre has a higher crystallinity than the as-spun fibre. Molecular orientation was also developed during hot-drawing as seen in Figures 3(a)-(c). Figure 3(a) shows the WAXD pattern of the fibre at the commencement of drawing and features one sharper ring on a diffused scattering ring. The diffused background ring indicates the presence of a non-crystalline (amorphous) phase while the sharper ring indicates that there are small randomly oriented crystallites also present. During stretching, the sharper ring developed into two arcs (see Figures 3(b) and (c)), characteristic of strain-induced crystallization and orientation [7].

Annealing can also enhance crystallization. Moreover, if the annealing is performed on a previously drawn fibre with its ends fixed, the additional crystallites which are formed tend to align themselves along the fibre axis [9, 10]. Figure 3(d) illustrates this annealing effect. The pattern in Figure 3(d) was obtained by annealing the drawn fibre (of which the XRD pattern is shown in Figure 3(c)) at 60°C for 10 min. As seen, more sharper spots appear in the pattern of the annealed fibre indicating enhanced crystallinity and orientation. When compared with the pattern in Figure 3(e), where the fibre was left to cool down to room temperature after hot drawing, the effect of annealing at the higher (60°C)

temperature is very clear. Therefore, both hot-drawing and annealing can be used to enhance crystallinity and orientation with the result that the fibre's tensile strength will be increased.

Figures 4(c) and (d) show the intensity profiles at different reciprocal lattice layers ($\ell = 0-10$) of X-ray scattering from the segmented triblock terpolymer and poly(L-lactide) fibres respectively. These intensity profiles correspond to the intensities in the patterns in Figures 4(a) and (b). The peak positions of the profiles for the segmented triblock terpolymer fibre are all very similar to those of the profiles for the poly(L-lactide) fibre, even though the spots on the scattering pattern of the segmented triblock terpolymer fibre are not well-defined, as seen in Figure 4(b). This indicates that the fibre is predominantly amorphous. It can be concluded that the crystal structure in the segmented triblock terpolymer fibre is the same as that in the poly(L-lactide) fibre. Poly(L-lactide) can crystallize in various crystal forms depending on the conditions of crystallization [11-13]. The XRD pattern of poly(L-lactide) in Figure 4(b) is shown to be of the α -form (pseudo-orthorhombic, $a = 10.6$, $b = 6.1$, and $c = 28.8$ Å) [14, 15], which is the most commonly encountered crystal form. Thus, the crystal structure in the segmented triblock terpolymer fibre is also of the α -form of poly(L-lactide).

4. CONCLUSIONS

A segmented triblock terpolymer of L-lactide, ϵ -caprolactone and glycolide with a composition ratio of 71:24:5 mol % was synthesized and spun into a monofilament fibre through an ice-water cooling bath. The as-spun fibre obtained was largely amorphous with low strength. Hot drawing was then employed to enhance the fibre's strength, as a result of which it was found that, by drawing the as-spun fibre at 60°C at a rate of 2500 %/min to $\lambda = 5.9$, its strength increased to 8 times that of the as-spun fibre. From the DSC and XRD experiments, the results showed clearly that both crystallinity and molecular orientation were induced by hot-drawing and

annealing and that the resultant oriented semi-crystalline morphology was responsible for the fibre's enhanced tensile strength. By comparing the XRD pattern of the drawn fibre with that of poly(L-lactide), it could be concluded that the terpolymer crystallized into the α -form of poly(L-lactide).

5. ACKNOWLEDGEMENTS

This work was supported by the National Metal and Materials Technology Center of Thailand (MTEC). One of us (W.C.) would like to thank the Thai Ministry of University Affairs and also both the Graduate School and the Faculty of Science of Chiang Mai University for their financial support.

REFERENCES

- [1] Kroschwitz, J. I., *Polymers : Biomaterials and Medical Applications*, New York: John Wiley & Sons, 1989.
- [2] Medical Devicelink, Synthetic Biodegradable Polymers as Medical Devices, <http://www.devicelink.com> (20/6/2001).
- [3] Cai Q., Bei J.Z. and Wang S.G., Synthesis and characterization of polycaprolactone (B)- poly(lactide-co-glycolide) (A) ABA block copolymer, *Polym. Adv. Technol.*, 2000; **11**: 159-166.
- [4] Baimark Y. and Molloy R., Synthesis and characterization of poly(L-lactide-co- ϵ -caprolactone) copolymers : Effects of stannous octoate initiator and diethylene glycol coinitiator concentrations, *Science Asia*, 2004; **30**: 327-334.
- [5] Baimark Y., Molloy R., Molloy N., Siripitayananon J., Punyodom W. and Sriyai M., Synthesis, characterization and melt spinning of a block copolymer of L-lactide and ϵ -caprolactone for potential use as an absorbable monofilament surgical suture, *J. Mater. Sci : Mater. Med.*, in press.
- [6] Fambri L., Pegoretti A., Fenner R., Incardona S.D. and Migliaresi C., Biodegradable fibres of poly(L-lactic acid) produced by melt spinning, *Polymer*, 1997; **38**: 79-85.
- [7] Toki S., Sics I., Ran S., Liu L., Hsiao B.S., Murakami S., Senoo K. and Kohjiya S., New Insights into Structure Development in Natural Rubber during Uniaxial Deformation by *in situ* Synchrotron X-ray Diffraction, *Macromolecules*, 2002; **35**: 6578 - 6584.
- [8] Toki S., Sics I., Ran S., Liu L. and Hsiao B.S., Molecular orientation and structural development in vulcanized polyisoprene rubbers during uniaxial deformation by *in situ* Synchrotron X-ray diffraction, *Polymer*, 2003; **44**: 6003-6011.
- [9] Tsuji H. and Ikada Y., Properties and morphologies of poly(L-lactide) : 1. Annealing condition effects on properties and morphologies of poly(L-lactide), *Polymer*, 1995; **36**: 2709-2716.
- [10] Medical Devicelink, The effects of annealing conditions on the structure and properties of polypropylene fibers, <http://www.devicelink.com/> (20/6/2001).
- [11] Eling B., Gogolewski S. and Pennings A. J., Biodegradable materials of poly(L-lactide acid):1. Melt-spun and solution-spun fibres, *Polymer*, 1982; **23**: 1587-1593.
- [12] Cartier L., Okihara T., Ikada Y., Tsuji H., Puiggali J. and Lotz B., Epitaxial crystallization and crystalline polymorphism of polylactides, *Polymer*, 2000; **41**: 8909-8919.
- [13] Sasaki S. and Asakura T., Helix distortion and crystal structure of the alpha-form of poly(L-lactide), *Macromolecules*, 2003; **36**: 8385-8390.
- [14] Hoogsteen A.W., Postema A.R., Pennings A.J., Brinke T.G. and Zugenmaier P., Crystal Structure, Conformation, and Morphology of Solution-spun Poly(L-lactide) Fibres, *Macromolecules*, 1990; **23**: 634-642.
- [15] Aleman C., Lotz B. and Puiggali J., Crystal Structure of the alpha-form of Poly(L-lactide), *Macromolecules*, 2001; **34**: 4795-4801.

VITA

Name	Wasinee Channuan
Date of Birth	24 April 1975
Academic Status	High School Certificate holder from Sukhothai Wittayakom, Sukhothai, 1993 B.Sc. and M.S. (Chemistry) degree holder from Chiang Mai University, Chiang Mai, 2001
Scholarship Awarded	Thai Ministry of University Affairs, 2001-2003 Graduate School, Chiang Mai University, 2005

ลิขสิทธิ์มหาวิทยาลัยเชียงใหม่
 Copyright © by Chiang Mai University
 All rights reserved